Award Number: W81XWH-12-1-0477

TITLE: Reducing toxicity of radiation treatment of advanced prostate cancer

PRINCIPAL INVESTIGATOR: Ulrich Rodeck, M.D., Ph.D.

CONTRACTING ORGANIZATION: Thomas Jefferson University, Philadelphia, PA 19107

REPORT DATE: October 2014

TYPE OF REPORT: Annual

PREPARED FOR: U.S. Army Medical Research and Materiel Command
Fort Detrick, Maryland 21702-5012

REPORT DOCUMENTATION PAGE

Form Approved
OMB No. 0704-0188

1. REPORT DATE	2. REPORT TYPE	3. DATES COVERED
October 2014	Annual	30 Sept 2013 – 29 Sept 2014

4. TITLE AND SUBTITLE

Reducing toxicity of radiation treatment of advanced prostate cancer

5a. CONTRACT NUMBER

5b. GRANT NUMBER
W81XWH-12-1-0477

5c. PROGRAM ELEMENT NUMBER

6. AUTHOR(S)
Ulrich Rodeck, MD, PhD

E-Mail: ulrich.rodeck@jefferson.edu

5d. PROJECT NUMBER

5e. TASK NUMBER

5f. WORK UNIT NUMBER

7. PERFORMING ORGANIZATION NAME(S) AND ADDRESS(ES)
Thomas Jefferson University
Philadelphia, PA 19107-5541

8. PERFORMING ORGANIZATION REPORT NUMBER

9. SPONSORING / MONITORING AGENCY NAME(S) AND ADDRESS(ES)

U.S. Army Medical Research and Materiel Command
Fort Detrick, Maryland 21702-5012

10. SPONSOR/MONITOR'S ACRONYM(S)

11. SPONSOR/MONITOR'S REPORT NUMBER(S)

12. DISTRIBUTION / AVAILABILITY STATEMENT

Approved for Public Release; Distribution Unlimited

13. SUPPLEMENTARY NOTES

14. ABSTRACT
Toxicity is a major impediment to effective radiation therapy of locally advanced prostate cancer. Work under this award focuses on the potential of a novel class of pharmacological 'radiation protectors' to reduce normal tissue toxicity of radiation therapy. During the second year of this award we focused on a particular compound (RTA 408) that had emerged as a robust and selective radiation protector of normal tissues. Importantly, this compound also showed anti-tumor activity against four human prostate cancer cell lines grown as xenotransplants in mice. Over the last year we have gained major insights into how this compound is likely to effect radiation protection of normal tissues. This work has centered on effects of the drug on myeloid (bone marrow-derived) cells with cytoprotective properties that are recruited into irradiated tissues. Ongoing work focuses on the characterization of the molecular targets within myeloid cells that contribute to the differential effects of this drug on normal and tumor tissues.

15. SUBJECT TERMS
Radiotherapy, Symptom Management, Signal Transduction, Drug Development

16. SECURITY CLASSIFICATION OF:			17. LIMITATION OF ABSTRACT	18. NUMBER OF PAGES	19a. NAME OF RESPONSIBLE PERSON
a. REPORT	b. ABSTRACT	c. THIS PAGE			USAMRMC
Unclassified	Unclassified	Unclassified	Unclassified	41	19b. TELEPHONE NUMBER *(include area code)*

Table of Contents

Page

1. INTRODUCTION:

Radiation therapy (RT) is a key therapeutic option for prostate cancer, either alone or in combination with hormone therapy. However, the radiation dose that can be safely administered is often lower than the dose considered to be optimal to eradicate tumor cells in the vicinity of the primary lesion, for example pelvic lymph nodes. This is due, in large part, to 'collateral damage' by radiation, i.e. toxicity to the intestine and the bladder. Treatment strategies to escalate the dose of radiation to the pelvic sentinel lymph nodes and/or the primary site, are limited by normal tissue dose constraints that can't be surmounted by IMRT or particle therapy. Hence protection of normal tissue will be a critical requirement for future dose escalation trials in patients with locally advanced disease. Existing radiation protectors including amifostine (1), sucralfate (2) and mesalazine (3) are of limited utility in selectively protecting the small and large intestines against radiation effects. This motivated us to explore the potential of a novel class of pharmacological 'radiation protectors' to reduce normal tissue toxicity associated with radiation therapy. In preliminary work we and others had identified several 'targeted agents', i.e. small molecule compounds which radioprotect multiple normal tissues including the epithelial lining of the intestinal tract against deleterious effects of high dose radiation. These included pharmacological inhibitors of NF-κB activity and inhibitors of glycogen synthase kinase(GSK)3 that mimic select pro-survival effects of the PI-3-kinase/AKT pathway (Table 1). Of note, the agents under investigation are modulators of signal transduction pathways and, thus, distinct from conventional ROS scavengers or antioxidants such as Amifostine. This is notwithstanding the fact that some of the inhibitors tested (e.g. ethyl pyruvate, CDDO) also exert antioxidant activity.

2. KEYWORDS:

Radiation therapy, symptom management, signal transduction, drug development

3. OVERALL PROJECT SUMMARY:

The compounds originally proposed for testing in the radiation protection setting are listed in Table 1. In the previous progress report we summarized data in support of the conclusions that (i) the synthetic oleanane triterpenoid RTA 408 is an effective radiation protector of normal tissues including the skin and the epithelial lining of the gastrointestinal system, (ii) among all of the compounds tested RTA 408 and EP are most effective when compared to the GSK inhibitors tested. (iii) radiation protection by RTA 408 is selective to normal tissues as growth of human prostate cancer xenotransplants is inhibited by RTA 408 either alone or in combination with ionizing radiation. These results have since been submitted for publication and are in press in Molecular Cancer Therapeutics (see Appendix). These results further encouraged us to focus during the last funding period on mechanisms of radiation protection provided by RTA 408. Of note these studies represent a logical extension of the original proposal but go far beyond the orginial goals and milestones.

Table 1: Compounds under investigation. The compounds indicated below were selected due to their radioprotective properties in zebrafish screens and in mice. All compounds used in zebrafish except RTA/CDDO were from Calbiochem/EMD. RTA 408 and other CDDO derivatives were provided by REATA Pharmaceuticals. Note that, in our previous progress report RTA 408 was referred to as TX425. Protection was achieved in zebrafish and mice at roughly equimolar concentrations where data are available in both model systems. Radioprotection of the GI system in zebrafish was selectively tested and observed for EP and CDDO as well as for LiCl, SB216763 and Azakenpaullone. Data were compiled from the following references (4-6). Zebrafish GSK3 inhibitor data from our laboratory are unpublished.

Pathway	Compound	Target(s)	Effective dose (in vitro)
NF-κB	Ethyl Pyruvate (EP)	NF-κBp65	1 mM
	RTA 408 (CDDO)	IKKβ/KEAP1-Nrf2	1 μM
GSK3	Lithium Chloride (LiCl)	GS3 (allosteric)	20 mM
	SB216763	GSK3 (ATP competitive)	5 μM
	Azakenpaullone	GSK3 (ATP competitive)	0.3 μM

1. Thiol modifying compounds of different chemical composition act as radiation protectors.

RTA 408 is a thiol-modifying compound (TMC) which is covalently interacts with free cysteines on the surface of proteins (7). While it effectively inhibits canonical activation of the NF-kB pathway (8) it also targets multiple other signaling intermediates and effectors (9-12). Previous work by us and others revealed that another thiol modifying agent, ethyl pyruvate (EP) also is an effective radiation protector (4, 5) and these results were confirmed by us (13).

Recently, yet another thiol-modifying compound (diaminoparthenolide (DMAPT)) was found to selectively radioprotect normal tissues while inhibiting tumor growth (14). Based on this recent report we directly compared radiation protection of mice by RTA 408 and DMAPT. This experiment revealed equipotent protection of mice against lethal gastrointestinal syndrome induced by 9 Gy total body radiation and the results achieved with either compounds are comparable with results obtained using the FDA-approved radiation protector amifostine (Fig. 1). In aggregate, these results support the hypothesis, that thiol-modifying agents of different chemical composition share a target spectrum that, in aggregate, underlies selective radiation protection of normal tissues. They provide the opportunity to identify shared targets relevant to either radiation protection of normal tissues or to anti-tumor effects of these agents.

Figure 1: Radioprotective effects of RTA 408 and DMAPT. (A) C57Bl/6 mice (n=5 per cohort) were administered RTA 408 (17.5 mg/kg i.p.) or DMAPT (at the concentrations indicated) or vehicle (DMSO) control 1 day and 1 hour prior to radiation exposure (8 Gy) followed by 3 daily doses post IR. Animals were euthanized at the end of the observation period, when weight loss reached or exceeded 20% of the initial weight, or if they showed signs of severe morbidity. (B) Radiation protection provided by RTA 408 as compared to Amifostine. Amifostine was administered once 1 h prior to radiation. RTA 408 was admininstered as described in the legend to panel (A).

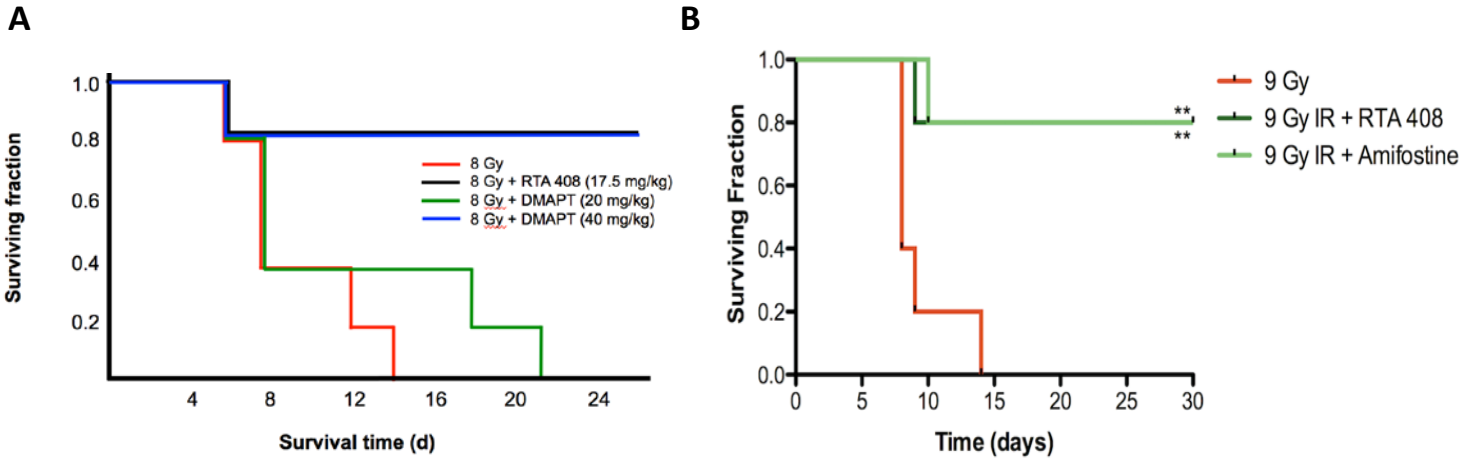

2. Effects of RTA 408 on normal and malignant cells in vitro.

Next, we determined whether we could recapitulate selective normal tissue protection by RTA 408 or DMAPT in human cells grown in vitro. This was done to establish an experimental platform for molecular target identification and validation as they relate to radiation protection. To this end, we determined the dose-dependent effects of either compound on survival and proliferation of primary normal epithelial cells (prostate cells and keratinocytes) as compared to prostate cancer cell lines. The prostate cancer cell lines tested were PC3, DU145, LNCaP-/C4-2B and CWR22Rv1 all of which are inhibited by RTA 408 when grown as xenografts in mice (13). Cell growth and survival were determined using both crystal violet staining of attached cells and WST assays measuring metabolic activity of cells. These assays were performed at least three times and an example for typical results using RTA 408 is shown in Fig. 2. Surprisingly, these assays revealed that, in contrast to our in vivo findings, the effects of RTA 408 and of DMAPT on normal and tumor cells grown in vitro were indistinguishable. In fact, both compounds inhibited survival and proliferation of normal and malignant

cells alike. Of note, this result is different from results published on DMAPT which reportedly selectively inhibits prostate cancer cells in vivo and vitro (14).

More importantly, these results indicate that the cytoprotective effects of RTA 408 and, most likely DMAPT, are not cell-autonomous but require the in vivo context and the interplay of different cell types provided only in vivo.

Figure 2: In vitro RTA 408 inhibtis survival and growth of normal and transformed cells equally.

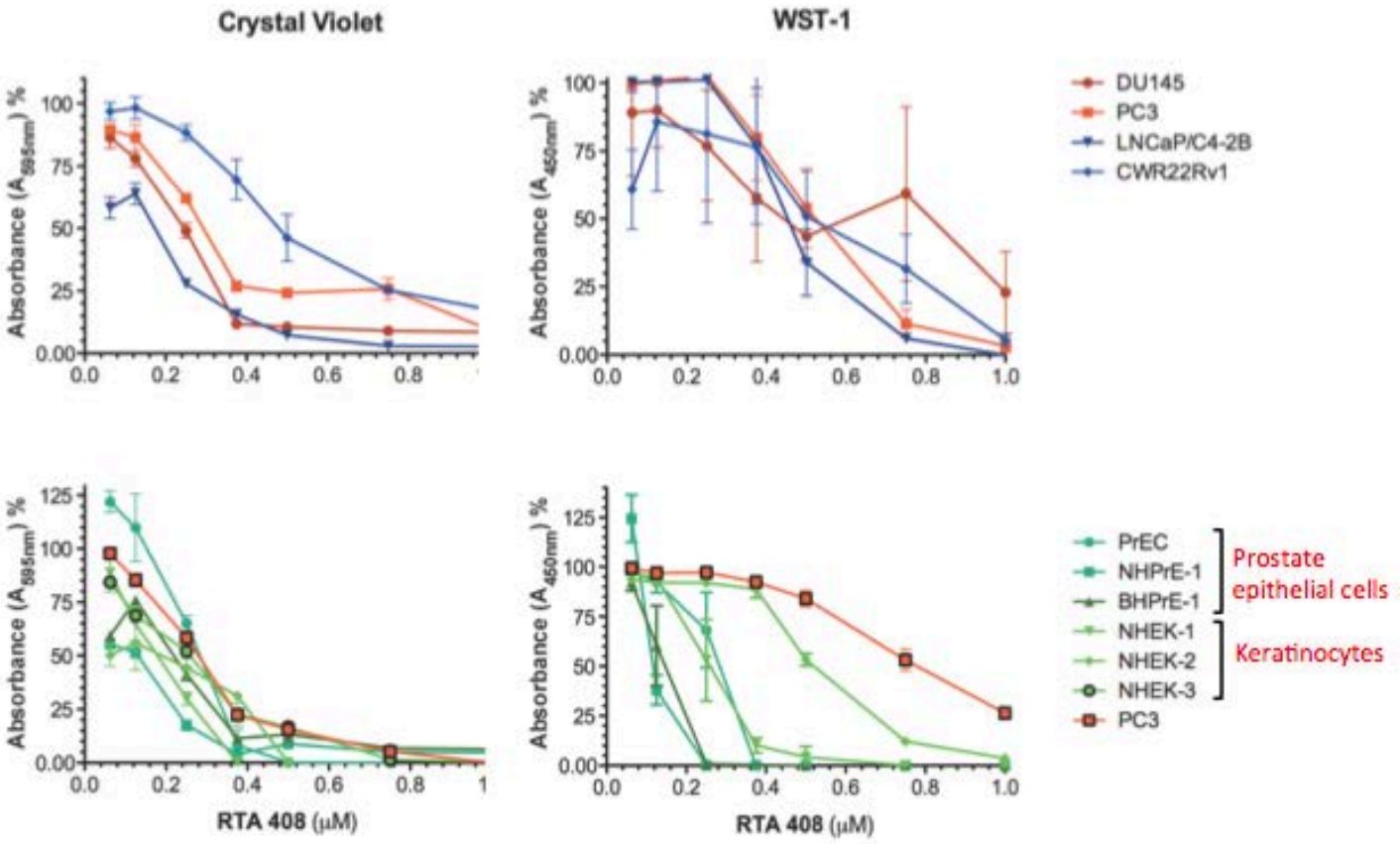

3. Radiation protection of the myeloid cell compartment by RTA 408

In a separate set of experiments we characterized cytoprotective effects of RTA 408 on the hematopoietic system. This was motivated by the observation that RTA 408-treated mice that survived radiation-induced gastrintestinal syndrome invariably continued to survive for more that 30 days indicative of survival of the hematopoietic syndrome as well.

In colaboration with Dr. William H. Fleming (Oregon Stem Cell Center; OSHU) we detemined that RTA 408 increased survival of hematopoietic raidation syndroma associated with complete rescue of functionally competent hematopoietic stem cells. Specifically, the administration of a brief course of RTA 408 treatment beginning 24 h after bone marrow lethal doses of radiation significantly increased overall survival. Importantly, treatment with RTA 408 led to the full recovery of steady state hematopoiesis with normalization of the frequency of hematopoietic stem and progenitor cells. Moreover, hematopoietic stem cells from RTA 408-mitigated mice showed lineage-balanced, long-term, multilineage potential as determined by serial bone marrow transplantation, indicative of their normal self-renewal activity. The potency of RTA 408 in mitigating radiation-induced bone marrow suppression makes it an attractive candidate for potential clinical use in treating both therapy-related and unanticipated radiation exposure. The results of this study have been submitted for publication and are currently under review (15).

4. RTA 408-dependent myeloid cell recruitment is required for survival and recovery from radiation-induced gastrointestinal syndrome.

Based on the results described in the preceding paragraph we asked whether bone marrow-derived cells contributed, in a non-cell autonomous fashion, to the rescue of GI syndrome. First, we established that treatment with RTA 408 leads to a dramatic influx of $CD11b^+$ myeloid cells into the irradiated lamina propria of the intestines (Fig. 3). This cell population is functionally relevant as a previous study showed that $CD11b^+$ cells provide radiation protection of the murine GI system in the bone marrow transplantation setting (16). In addition and more importantly, depletion of these cells by treatment of mice with an antibody blocking CD11b (M1/70 (17)) completely abrogated radiation protection of mice by RTA 408 (Fig. 4). Collectively, these results support the hypothesis that RTA 408 effects radiation protection of normal epithelial tissues by rescuing, recruiting and/or reprogramming myeloid cells with cytoprotective properties. Characterizing this mechanism further is at the center of our research effort going into the third year of funding through this award.

Figure 3: RTA 408 recruits $CD11b^+$ myeloid cells into the irradiated GI tract. (A) Increased abundance of $CD11b^+$ cells in irradiated (9 Gy) intestines of mice treated with RTA 408. (B) Flow cytometric analysis of $CD11b^+$ cells in irradiated (9 Gy) intestines of mice treated with RTA 408. Representative results from one mouse are shown. Note increased number of $CD11b^{hi}/CD11c^{med}$ immunocytes in the irradiated mouse receiving RTA 408.

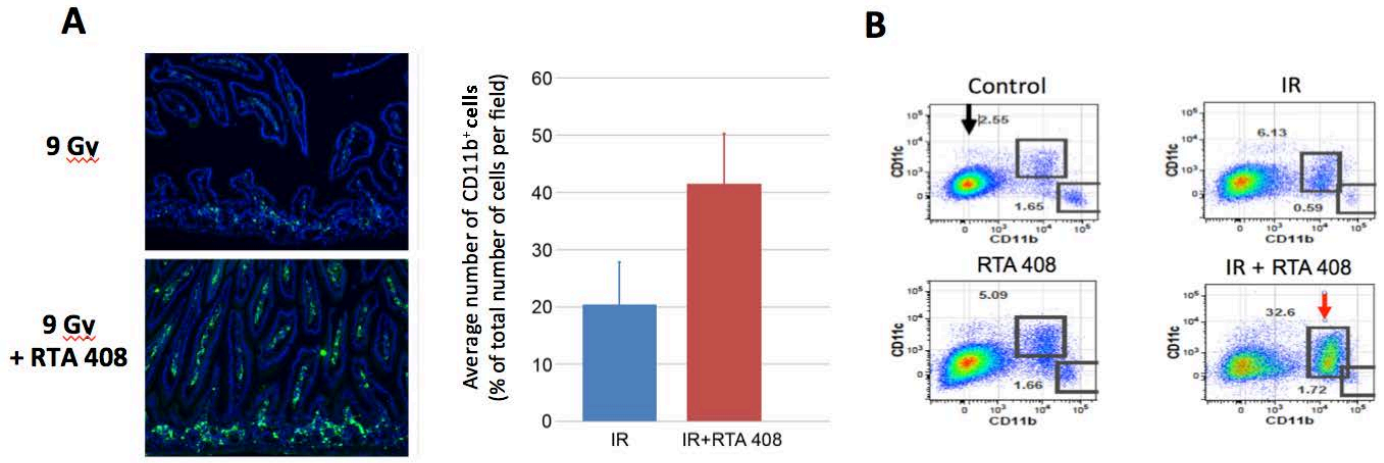

Figure 4: Recruitment of $CD11b^+$ myeloid cells into the irradiated GI tract is required for radiation portection by RTA 408. Prior to irradiation and drug treamtent mice were pretreated with the CD11b blocking antibody M1/70. Blocking recruitment of $CD11b^+$ cells abrogated radiation protection by RTA 408.

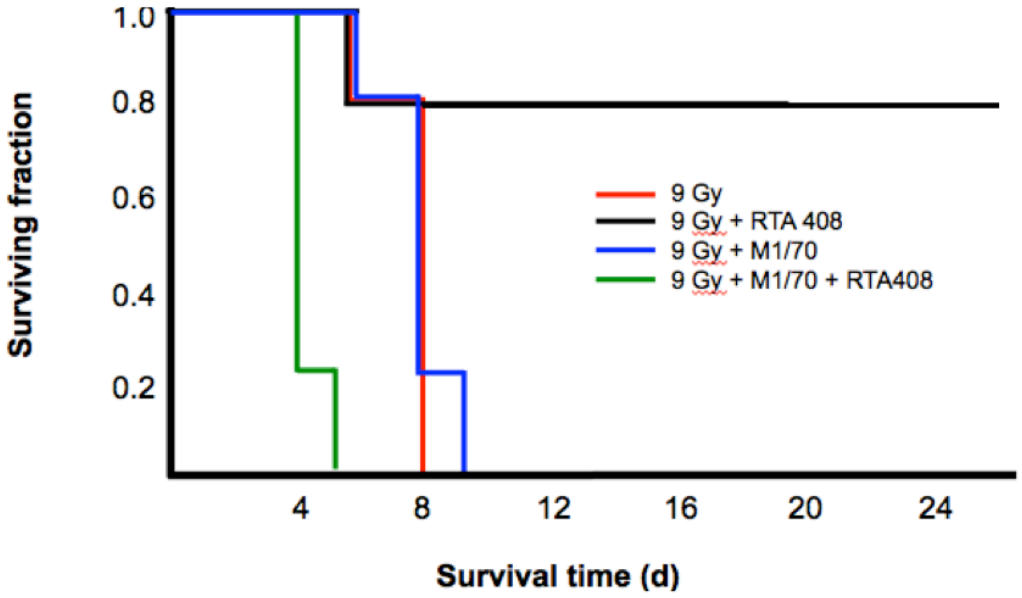

4. KEY RESEARCH ACCOMPLISHMENTS:

- Identified RTA 408 as a lead compound to be further characterized and developed as a selective radiation protector.
- Established a novel mechanism of action of RTA 408 (and potentially other radioprotective thiol-modifying compounds) related to rescue, recruitment and reprogramming myeloid cells to sites of tissue injury.

5. CONCLUSION:

We have established that the thiol-modifying compound RTA 408 is a robust radiation protector of multiple cell types and organ systems (hematopoietic, skin and gastrointestinal) in mice. Preliminary results point to a previously unrecognized mechanism of action of radiation protectors that depends on reprograming myeloid cells. Identification of relevant molecular targets of RTA 408 and related compounds in these myeloid cells is imperative as a corollary to further drug development. This investigation will be continued during the next funding period. Of note, during the last funding period, REATA Pharmaceuticals has begun a clinical trial (NCT02142959) to explore utility of a topical formulation of RTA 408 as a protector against radiation dermatitis. In summary, the work performed under this award during the last 2 years has provided unique insights into radiation protection mechanisms amenable to pharmacological intervention and has contributed to the initiation of a clinical trial of RTA 408 as a radioprotector.

6. PUBLICATIONS, ABSTRACTS, AND PRESENTATIONS:

- Invited oral presentation at the 20th Annual Prostate Cancer Foundation Retreat in October 2013.
- Invited oral presentation at the NIH-NIAID “Centers for Medical Countermeasures Against Radiation” Workshop, Baltimore October 2014.
- Invited to submit a full project as part of the competing renewal application for the Center of Countermeasures against Radiation; NIH/NIAID) at Einstein Medical Center, Bronx, NY (PI: Dr. C. Guha).
- Published one manuscript describing selective radiation protection of gastrointestinal epithelium by a compound (RTA 408) that has anti-tumor properties (Alexxeev et al.).

- Submitted a second manuscript on RTA 408-dependent protection of hematopoietic cells against radiation damage (Goldman et al.).
- A third manuscript on effects of RTA 408 on myeloid cell phenotypes is in preparation.

7. INVENTIONS, PATENTS AND LICENSES:
N/A

8. REPORTABLE OUTCOMES:

This award has led to unique insights into the mechanism of action by which certain thiol modifying agents with anti-tumor properties provide selective radiation protection to normal tissues. Of note, the lead compound identified in the conduct of our work has already enteered clinical trials not only as an anti-tumor agent but also as a protector against radiation damage to the skin of cancer patients undergoing radiation therapy.

9. OTHER ACHIEVEMENTS:

Results obtained through this award have contirbuted to submission of two grant applications to the NIH. One application is an RO1 application to further elucidate how RTA 408 and related compounds affect myeloid cell physiology and phenotype. The second application is a project incorporated into the resubmission to NIH/NIAID of a U19 grant to continue funding of a "Center for Medical Countermeasures against Radiation" (PI: Chandan Guha).

10. REFERENCES:

1. Simone, N.L., Menard, C., Soule, B.P., Albert, P.S., Guion, P., Smith, S., Godette, D., Crouse, N.S., Sciuto, L.C., Cooley-Zgela, T., et al. 2008. Intrarectal amifostine during external beam radiation therapy for prostate cancer produces significant improvements in Quality of Life measured by EPIC score. *International Journal of Radiation Oncology, Biology, Physics* 70:90-95.
2. Hovdenak, N., Sorbye, H., and Dahl, O. 2005. Sucralfate does not ameliorate acute radiation proctitis: randomised study and meta-analysis. *Clinical Oncology* 17:485-491.
3. Sanguineti, G., Franzone, P., Marcenaro, M., Foppiano, F., and Vitale, V. 2003. Sucralfate versus mesalazine versus hydrocortisone in the prevention of acute radiation proctitis during conformal radiotherapy for prostate carcinoma. A randomized study. *Strahlenther Onkol* 179:464-470.
4. Epperly, M., Jin, S., Nie, S., Cao, S., Zhang, X., Franicola, D., Wang, H., Fink, M.P., and Greenberger, J.S. 2007. Ethyl pyruvate, a potentially effective mitigator of damage after total-body irradiation. *Radiation Research* 168:552-559.
5. Daroczi, B., Kari, G., Ren, Q., Dicker, A.P., and Rodeck, U. 2009. Nuclear factor kappaB inhibitors alleviate and the proteasome inhibitor PS-341 exacerbates radiation toxicity in zebrafish embryos. *Molecular Cancer Therapeutics* 8:2625-2634.
6. Thotala, D.K., Geng, L., Dickey, A.K., Hallahan, D.E., and Yazlovitskaya, E.M. 2010. A new class of molecular targeted radioprotectors: GSK-3beta inhibitors. *International Journal of Radiation Oncology, Biology, Physics* 76:557-565.
7. Yue, P., Zhou, Z., Khuri, F.R., and Sun, S.Y. 2006. Depletion of intracellular glutathione contributes to JNK-mediated death receptor 5 upregulation and apoptosis induction by the novel synthetic triterpenoid methyl-2-cyano-3, 12-dioxooleana-1, 9-dien-28-oate (CDDO-Me). *Cancer biology & therapy* 5:492-497.
8. Shishodia, S., Sethi, G., Konopleva, M., Andreeff, M., and Aggarwal, B.B. 2006. A synthetic triterpenoid, CDDO-Me, inhibits IkappaBalpha kinase and enhances apoptosis induced by TNF and chemotherapeutic agents through down-regulation of expression of nuclear factor kappaB-regulated gene products in human leukemic cells. *Clinical Cancer Research* 12:1828-1838.
9. Yore, M.M., Kettenbach, A.N., Sporn, M.B., Gerber, S.A., and Liby, K.T. 2011. Proteomic analysis shows synthetic oleanane triterpenoid binds to mTOR. *PLoS One* 6:e22862.
10. Pitha-Rowe, I., Liby, K., Royce, D., and Sporn, M. 2009. Synthetic triterpenoids attenuate cytotoxic retinal injury: cross-talk between Nrf2 and PI3K/AKT signaling through inhibition of the lipid phosphatase PTEN. *Investigative ophthalmology & visual science* 50:5339-5347.

11. Liu, Y., Gao, X., Deeb, D., and Gautam, S.C. 2012. Oleanane triterpenoid CDDO-Me inhibits Akt activity without affecting PDK1 kinase or PP2A phosphatase activity in cancer cells. *Biochem Biophys Res Commun* 417:570-575.
12. Ji, Y., Lee, H.J., Goodman, C., Uskokovic, M., Liby, K., Sporn, M., and Suh, N. 2006. The synthetic triterpenoid CDDO-imidazolide induces monocytic differentiation by activating the Smad and ERK signaling pathways in HL60 leukemia cells. *Molecular Cancer Therapeutics* 5:1452-1458.
13. Alexeev, V., Lash, E., Aguillard, A., Corsini, L., Bitterman, A., Ward, K., Dicker, A.P., A, L., and Rodeck, U. 2014. Radiation protection of the gastrointestinal tract and growth inhibition of prostate cancer xenografts by a single compound (in press).
14. Xu, Y., Fang, F., Miriyala, S., Crooks, P.A., Oberley, T.D., Chaiswing, L., Noel, T., Holley, A.K., Zhao, Y., Kiningham, K.K., et al. 2013. KEAP1 Is a Redox Sensitive Target That Arbitrates the Opposing Radiosensitive Effects of Parthenolide in Normal and Cancer Cells. *Cancer Res* 73:4406-4417.
15. Goldman, D.C., Alexeev, V., Lash, E., Guha, C., Rodeck, U., and Fleming, W.H. 2014. The triterpenoid RTA 408 is a robust mitigator of hematopoietic acute radiation syndrome in mice. *(submitted)*.
16. Saha, S., Bhanja, P., Kabarriti, R., Liu, L., Alfieri, A.A., and Guha, C. 2011. Bone marrow stromal cell transplantation mitigates radiation-induced gastrointestinal syndrome in mice. *PLoS One* 6:e24072.
17. Welt, F.G., Edelman, E.R., Simon, D.I., and Rogers, C. 2000. Neutrophil, not macrophage, infiltration precedes neointimal thickening in balloon-injured arteries. *Arterioscler Thromb Vasc Biol* 20:2553-2558.

11. APPENDICES:

We have included pdf files of the two manuscripts referred to above. Manuscript #1 (Alexeev et al) is in press in Molecular Cancer Research, manuscript #2 (Goldman et al) is currently under review in Radiation Research.

Small Molecule Therapeutics

Molecular Cancer Therapeutics

Radiation Protection of the Gastrointestinal Tract and Growth Inhibition of Prostate Cancer Xenografts by a Single Compound

Vitali Alexeev[1], Elizabeth Lash[1], April Aguillard[1], Laura Corsini[1], Avi Bitterman[1], Keith Ward[2], Adam P. Dicker[3], Alban Linnenbach[1], and Ulrich Rodeck[1,3]

Abstract

Normal tissue toxicity markedly reduces the therapeutic index of genotoxic anticancer agents, including ionizing radiation. Countermeasures against tissue damage caused by radiation are limited by their potential to also protect malignant cells and tissues. Here, we tested a panel of signal transduction modifiers for selective radioprotection of normal but not tumor tissues. These included three inhibitors of GSK3 (LiCl, SB216763, and SB415286) and two inhibitors of NF-κB (ethyl pyruvate and RTA 408). Among these, the thiol-reactive triterpenoid RTA 408 emerged as a robust and effective protector of multiple organ systems (gastrointestinal, skin, and hemopoietic) against lethal doses of radiation. RTA 408 preserved survival and proliferation of crypt cells in lethally irradiated small intestines while reducing apoptosis incidence in crypts and villi. In contrast, RTA 408 uniformly inhibited growth of established CWR-22Rv1, LNCaP/C4-2B, PC3, and DU145 xenografts either alone or combined with radiation. Anti-tumor effects in vivo were associated with reduced proliferation and intratumoral apoptosis and with inhibition of NF-κB–dependent transcription in PC3 cells. Selective protection of normal tissue compartments by RTA 408 critically depended on tissue context and could not be replicated *in vitro*. Collectively, these data highlight the potential of RTA 408 as a cytoprotective agent that may be safely used in chemoradiation approaches. *Mol Cancer Ther; 1–10. ©2014 AACR.*

Introduction

Radiotherapy is the most common therapeutic modality across a wide range of malignant diseases, including prostate cancer. However, the delivery of curative radiation doses is hampered by acute or chronic "collateral damage" affecting normal tissues. When treating tumors in the abdominal cavity, toxicity to the intestine and the bladder are often dose limiting (1). Highly targeted methods to deliver radiation specifically to disease sites alleviate radiation toxicity, yet 40% to 50% of patients with locally advanced prostate cancers recur locally following treatment (2). Hence, protection of normal tissue will be a critical element of future dose-escalation trials in patients with locally advanced prostate cancer. Existing radiation protectors, including amifostine (3), are of limited utility in protecting the small and large intestines against radiation effects.

Inflammation is a key element of the radiation response of normal and tumor tissues and is commonly associated with increased activity of NF-κB (4, 5). Previously, we demonstrated that several inhibitors of canonical NF-κB activation improved survival of lethally irradiated zebrafish embryos and preserved gastrointestinal morphology and function (6). Inhibitors of glycogen synthase kinase (GSK)3 similarly protect normal tissues, including the gastrointestinal tract (7, 8). While the role of GSK3β in cell stress responses is complex (for review, see ref. 9), it has been implicated in modifying NF-κB–dependent transcription of genes encoding proinflammatory proteins (10, 11).

Here, we performed a side-by-side comparison of radioprotective properties of five compounds targeting either GSK3 and/or NF-κB with a focus on the gastrointestinal tract. We report that the triterpenoid RTA 408 provides robust radiation protection to the gastrointestinal system of mice and markedly improves overall survival of lethally irradiated mice. Importantly, normal tissue protection by RTA 408 is contrasted by inhibition of human prostate cancer xenograft growth in mice.

Materials and Methods

Materials and cells

Compounds were obtained from the following sources: Ethyl pyruvate and lithium chloride (Sigma-Aldrich), SB216763 and SB416583 (Tocris Bioscience), amifostine (Medimmune), and 2-cyano-3,12- dioxooleana-1,9

[1]Department of Dermatology, Thomas Jefferson University, Philadelphia, Pennsylvania. [2]REATA Pharmaceuticals, Irving, Texas. [3]Department of Radiation Oncology, Thomas Jefferson University, Philadelphia, Pennsylvania.

Note: Supplementary data for this article are available at Molecular Cancer Therapeutics Online (http://mct.aacrjournals.org/).

Corresponding Author: Ulrich Rodeck, Thomas Jefferson University, 233 S 10th Street, Philadelphia, PA 19130. Phone/Fax: 215-503-5622; E-mail: ulrich.rodeck@jefferson.edu

doi: 10.1158/1535-7163.MCT-14-0354

(11)-dien-28-oic acid (CDDO) derivative RTA 408 (REATA Pharmaceuticals). Prostate cancer cells (PC3, LNCaP/C4-2B, DU145, and CWR-22Rv1) were originally obtained from ATCC or from Dr. Thomas Pretlow (Case Western Reserve University, Cleveland, OH) and generously provided by Dr. Marja Nevalainen (Thomas Jefferson University, Philadelphia, PA), and immortalized NHPrE-1 and BHPrE-1 prostate epithelial cells were a gift from Dr. Simon Hayward (Vanderbilt University Medical Center, Nashville, TN). Normal primary prostate epithelial cells (PrEC) were from Lonza. The prostate cancer cell lines were authenticated on a regular basis by monitoring cell morphology, androgen responsiveness, and the expression of cell line–specific markers. Normal primary epidermal keratinocyte cultures were established using standard protocols. Cells were routinely tested for mycoplasma contamination using MycoSensor PCR Assay Kit (Stratagene). Tumor cells were grown in RPMI1640 supplemented with 10% FBS (Corning Cellgro). Normal and immortalized prostate epithelial cells and primary keratinocytes were grown in specialty media (Lonza). For *in vivo* imaging, PC3 prostate carcinoma cells were stably transfected with reporter plasmids [pGL4.51(luc2/CMV/Neo) and pNL3.2.NF-κB-RE(NlucP/NF-κB-RE/Hygro), Promega] encoding firefly luciferase (FLuc) and NanoLuc luciferase, respectively, and luciferase reporter activity tested using reporter-specific *in vitro* assays (Promega).

Toxicity studies in mice

C57Bl/6 mice (6–8 weeks old) were from Charles River Laboratories. Mice were kept in pathogen-free conditions and handled in accordance with the requirements of the Guidelines for Animal Experiments and after approval of the experimental protocols by the Institutional Animal Care and Use Committee of Thomas Jefferson University (Philadelphia, PA). Ionizing radiation (IR) was administered at doses ranging from 5 to 30 Gy using a 250-kVp X-ray machine (PanTak) with 50-cm source-to-skin distance and a 2-mm copper filter. The dose rate was approximately 1.4 Gy/minute. Drugs were uniformly administered by intraperitoneal injection for up to 2 days before IR treatment, and on days 1, 2, and 3 after IR treatment as indicated. For comparison of RTA 408 and amifostine, mice received one dose (17.5 mg/kg) of RTA 408 24 hours before IR (whole body, 9 Gy), one dose 1 hour before IR, and 2 additional doses 24 and 48 hours after IR; amifostine was injected once (250 mg/kg) 15 minutes before IR. All injections were done intraperitoneally. Animals were euthanized at the end of the observation period, or when weight loss reached or exceeded 20% of the initial weight, or if they showed signs of severe morbidity (lethargy, hunched posture, and/or shivering or severe diarrhea). Kaplan–Meier survival curves were compared by using the log-rank (Mantel–Cox) test.

Growth inhibition of prostate cancer xenografts

Prostate carcinoma cells were inoculated by subcutaneous injection (5×10^6 per mouse) into the lower abdominal skin of male *Foxn1nu* (nude) mice (6–8 weeks old; Charles River Laboratories). Tumor progression was monitored by caliper measurements and by *in vivo* live imaging (see below). Xenografts were allowed to grow for 2 to 3 weeks before treatment. RTA 408 (17.5 mg/kg) or vehicle control (DMSO) were administered intraperitoneally three times per week until the end of the observation periods. To assess effects of the combination of RTA 408 and IR, radiation (5 Gy) was administered at different time points as indicated. Tumor volumes were calculated by multiplying the two longest planar axes measured by the depth of the tumor (as determined by caliper measurements). Mixed effects regression models were used to determine statistical significance of tumor growth data over time.

In situ imaging of xenografts and image analysis

For FLuc-based *in vivo* live imaging, mice were injected intraperitoneally with 200 μL D-luciferin in PBS (15 mg/mL) per 20 g of mouse body weight 15 minutes before imaging, and imaged using an IVIS In Vivo Imaging System (Caliper Life Sciences). For *in vivo* imaging of the NanoLuc luciferase under the control of the NF-κB response element, 100 μL of the NanoGlo substrate (10 μg; Promega) were injected via tail vein. Image analysis and quantitation was done using Living image 4.2 software (Caliper LifeSciences). Luciferase-positive areas on individual images were selected as regions of interest (ROI) with a 14% threshold. Planar spectral images were automatically analyzed by the software. Total counts for all pixels inside the ROI were recorded. At least 3 animals from each experimental group were used for each time point.

Histology, immunohistochemistry, and *in situ* apoptosis detection

For histologic, immunofluorescent, and direct fluorescent analyses, tissue samples (e.g., small intestines, tumors) were embedded in the optimal cutting temperature compound (Tissue-Tek), and cryosectioned (7 μm). Hematoxylin and eosin staining was done on ethanol/acetic acid–fixed slides. Apoptosis incidence was determined by terminal deoxynucleotidyl transferase dUTP nick end labeling (TUNEL) using the *In Situ* Cell Death Detection Kit (Roche Applied Science) and 4′,6-diamidino-2-phenylindole (DAPI) counterstain. Quantitative analysis was done using ImagePro software (Media Cybernetics) on at least 6 different and independent microscopic fields for each treatment condition. Indirect immunofluorescence was performed by incubation with primary antibodies for cleaved PARP (Asp214) Human Specific (Cell Signaling Technology), M30CytoDEATH (Roche Applied Science), or Ki-67 (Abcam) for 1 hour at room temperature or overnight at 4°C followed by secondary antibodies labeled with either Alexafluor 488 or Alexafluor 594 (BD Biosciences). Sections were counterstained with DAPI and slides were mounted using antifade Fluorosafe reagent (Calbiochem).

In vitro cell growth and viability assays

Cells were seeded in 96-well plates at 15,000 cells per well; after 24 hours, RTA 408 or vehicle were added in triplicate. After 72 hours, attached cells were fixed with 70% ethanol, stained with crystal violet solution (0.2% crystal violet in 2% ethanol), and quantitated by measuring absorbance (OD_{A595}). Metabolic activity was determined after 72 hours by addition of WST-1 reagent (Roche; 10 μL per 100 μL supernatant) for at least 3 hour at 37ºC, followed by measuring absorbance at OD_{A450} with a reference of OD_{A650} and using wells containing media without cells for background subtraction. Statistical differences between treatment groups were determined using one-way ANOVA with Tukey posttest correction (GraphPad Prism).

Immunoblot analyses

Prostate carcinoma cell lines were treated for 24 hours with RTA 408 or vehicle at the concentrations indicated. Immunoblots were reacted with (i) PARP-1 primary antibody (C2-10; Santa Cruz Biotechnology) and IRDye 800CW goat anti-mouse IgG1-specific secondary antibody; (ii) cleaved caspase-3 (Asp175; 5A1E) primary antibody (Cell Signaling Technology) and IRDye 800CW Donkey anti-Rabbit IgG (H + L) secondary antibody; (iii) cleaved caspase-8 (Asp384; 11G10) primary antibody (Cell Signaling Technology) and IRDye 800CW goat anti-mouse IgG1-specific secondary antibody, or (iv) M30CytoDEATH primary antibody (Roche Applied Science) and IRDye 800CW Goat anti-mouse IgG2b-specific secondary antibody; all secondary antibodies were from LICOR. Filters were analyzed on a LICOR Odyssey imaging system.

Colony formation assays

Cells were seeded at clonogenic densities in T-25 flasks and treated with RTA 408 at various concentrations or DMSO, at 24 and 1 hour before radiation exposure. IR was administered at 0, 2, 4, 6, and 8 Gy. All treatments were performed in biologic triplicate. After IR, flasks were incubated for 2 weeks. Colonies were identified by crystal violet staining; those containing ≥50 cells were counted. The data were fit to a linear quadratic model for cell survival by using GraphPad Prism software and the equation $Y = \exp(-a \times x - b \times x^2)$ (12). Statistically significant differences between drug and control curves were determined by using two-way ANOVA.

Results and Discussion

Inhibitors of canonical NF-κB activation and of GSK3 improve survival of lethally irradiated mice

We performed a side-by-side comparison of several NF-κB and GSK3 inhibitors on mice challenged with a

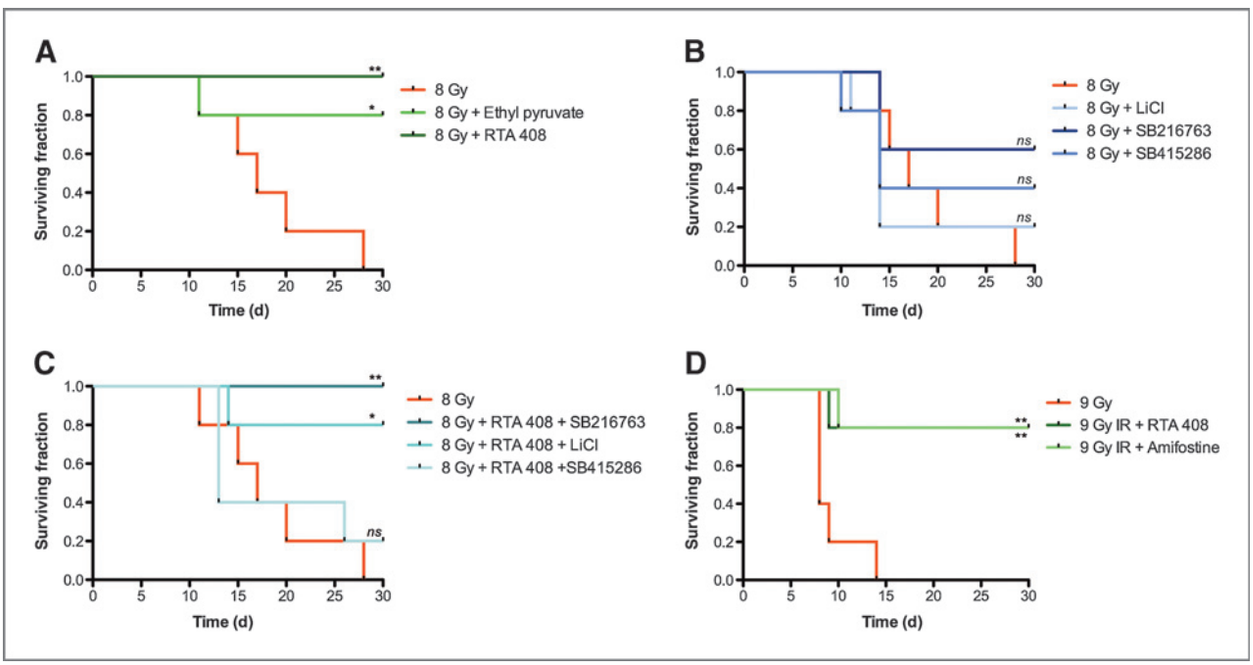

Figure 1. Effects of signal transduction modifiers on survival of lethally irradiated mice. A, survival of mice pretreated (24 hours) with the NF-κB inhibitors ethyl pyruvate (EP; 70 mg/kg) or RTA 408 (17.5 mg/kg) and receiving 8 Gy single dose whole body radiation. Ethyl pyruvate was administered 15 minutes before IR and on days 1 to 3 after IR. RTA 408 was administered 1 day and 1 hour preirradiation and on days 1 to 3 after IR. B, survival of mice treated with the GSK3 inhibitors LiCl (40 mg/kg), SB415286 (1 mg/kg), and SB216673 (1 mg/kg) and receiving 8 Gy single dose whole body radiation; treatment schedule for these compounds was 2 and 1 day before IR and daily on days 1 to 3 after IR. C, effects of select combinations of NF-κB and GSK3 inhibitors on survival of irradiated mice (8 Gy); treatment schedules for individual compounds as described under A. D, survival of irradiated mice (whole body, 9 Gy) treated with RTA 408 (17.5 mg/kg) at 24 and 1 hour before IR and on days 1 to 2 after IR or with amifostine (250 mg/kg) administered 15 minutes before IR. Experimental groups in each panel consisted of 5 animals each. *P* value summaries refer to pairwise comparisons between IR and (IR + drug) treatment groups, generated by using the log-rank (Mantel–Cox) test.

lethal whole body radiation dose (8 Gy; Fig. 1). All of the compounds reportedly protect against or mitigate radiation injury in different experimental settings either *in vitro* or *in vivo*. They included two inhibitors of canonical NF-κB signaling (ethyl pyruvate; ref. 13) and RTA 408 (ref. 14; Fig. 1A), and three GSK3 inhibitors, including lithium chloride (LiCl; ref. 8), SB415286 (8), and SB216763 (ref. 8; Fig. 1B, c). Ethyl pyruvate interferes with NF-κBp65 signaling by covalently modifying a reactive cysteine residue (Cys36) of the NF-κBp65 subunit (15). RTA 408 is a variant of the triterpenoid CDDO that reversibly and covalently modifies reactive cysteine residues on multiple proteins, including several of potential relevance to radiation protection. Specifically, binding of CDDO to Cys179 in IKKβ leads to inhibition of canonical NF-κB signaling (16) and binding to KEAP1 leads to increased levels of the transcription factor Nrf2 and of multiple antioxidant and phase II defense enzymes (17). RTA 408 was included in the screen because we previously observed robust radioprotection of zebrafish embryos by another variant of CDDO (CDDO-TFEA; ref. 6). SB415286 and SB216763 are ATP-competitive GSK3 inhibitors (18), whereas LiCl increases inhibitory phosphorylation of GSK3 (19). To allow direct side-by-side comparison all drugs were given using a standardized regimen, i.e., for 1 day and 1 hour before radiation and daily for 3 days after. Drug dosages were guided by published results and administration was by intraperitoneal injection. We observed various levels of radiation protection with each of the compounds tested. The CDDO derivative RTA 408 provided robust and consistent levels of radiation protection [100% at 30 days post-IR (8 Gy)] either as a single compound (Fig. 1A) or in combination with the GSK3 inhibitor SB216763 (Fig. 1C). In agreement with an earlier report (13), ethyl pyruvate also markedly increased survival of lethally irradiated mice (Fig. 1A). Interestingly, the survival advantage provided by RTA 408 was compromised when combined with SB415286 but not when combined with SB216763 (Fig. 1C). Similarly, survival of lethally irradiated mice treated with a combination of RTA 408 and LiCl was slightly lower than survival of mice receiving RTA 408 alone (Fig. 1C). Finally, RTA 408 produced levels of radiation protection similar to amifostine, the only currently approved radiation protector (Fig. 1D). These results encouraged us to further investigate tissue protection provided by RTA 408 alone.

RTA 408 protects mice against gastrointestinal syndrome and death after lethal doses of radiation

Next, we investigated the effect of RTA 408 on the small intestine in C57Bl/6 mice irradiated at a dose (9 Gy) that causes death from gastrointestinal syndrome within 10 to 15 days (20). We observed that RTA 408 preserved the integrity of the mucosal lining of the small intestine of

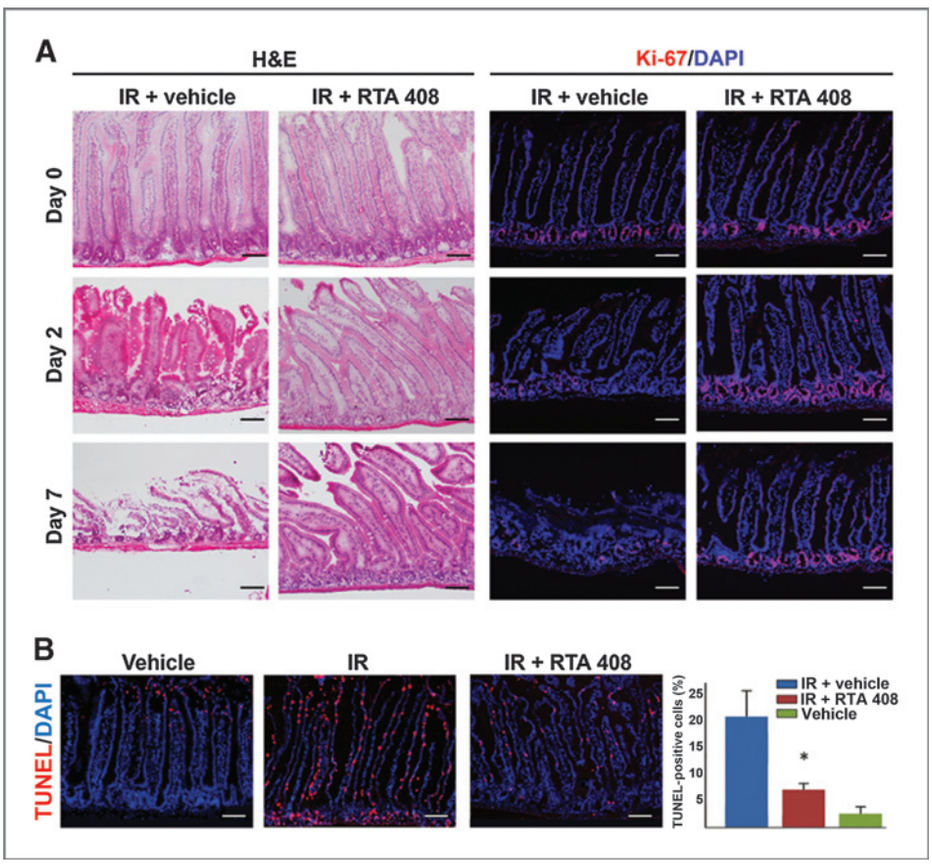

Figure 2. RTA 408 reduces radiation-associated damage to the mucosal lining of the small intestine after single dose (9 Gy) radiation exposure. RTA 408 (17.5 mg/kg) was administered on days 1 to 3 after IR. A, assessment of gastrointestinal morphology was performed on tissue sections sampled days 2 and 7 after radiation exposure. Parallel sections were subjected to staining with Ki-67–reactive antibody to ascertain the proliferative state of the gastrointestinal stem cell compartment located in the crypt areas; scale bars = 100 μm. B, effects of RTA 408 on radiation-induced apoptosis incidence in the gastrointestinal mucosa. RTA 408 (17.5 mg/kg) was administered 24 hours after IR (9 Gy) and small intestine tissues sampled at 48 hours. Apoptosis incidence was determined by TUNEL staining and cell nuclei were counterstained with DAPI; scale bars = 100 μm. Results shown in D represent mean ± SD of at least 6 fields per condition analyzed. The number of TUNEL-positive cells was significantly (Student *t* test; $P < 0.05$) reduced in irradiated animals receiving RTA 408 when compared with vehicle-treated, irradiated animals.

lethally irradiated mice (Fig. 2A). Mice that did not succumb to gastrointestinal syndrome lived beyond 30 days after IR, consistent with radiation protection of multiple organs, including the hemopoietic system. Furthermore, as determined by Ki-67 staining RTA 408-treated mice revealed robust proliferation in the crypt area at 2 and 7 days after IR, whereas radiation alone (9 Gy) markedly reduced proliferation in this tissue compartment concurrent with extensive tissue destruction (Fig. 2A). RTA 408 also significantly reduced radiation-induced apoptosis in both villi and crypts as determined by TUNEL staining (Fig. 2B). This effect extended to the skin, in which RTA 408 similarly reduced the apoptosis incidence caused by radiation exposure (Supplementary Fig. S1).

RTA 408 inhibits cell growth and survival of human prostate cancer *in vivo*

To address whether the cytoprotective effects of RTA 408 extended to tumor cells, we first tested the effects of RTA 408 on four different prostate cancer cell lines

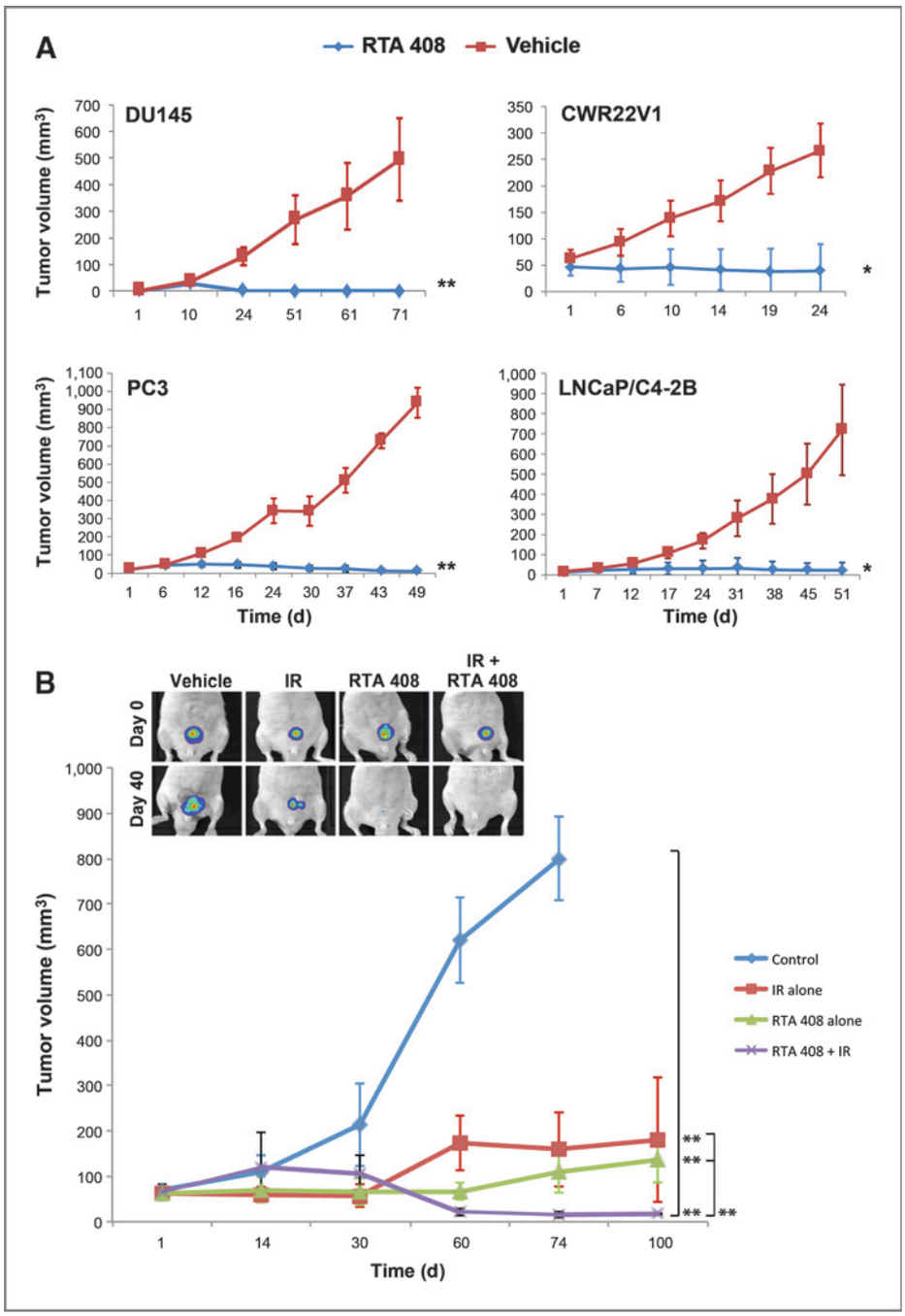

Figure 3. RTA 408 inhibits growth and survival of human prostate cancer xenotransplants. A, effects of RTA 408 on growth of DU145, PC3, LNCaP/C4-2B, and CWR22Rv1 cells *in vivo*. RTA 408 was administered (3 times per week at 17.5 mg/kg) after tumors had reached volumes exceeding 25 to 30 mm^3. Experimental groups consisted of 5 animals each. Results represent mean ± SD of these groups. *P* value summaries refer to tumor growth trajectories over time in RTA 408 and control groups. B, inhibition of PC3 xenograft growth and survival by combined radiation and RTA 408 treatment. Tumor-bearing mice were treated for 2 weeks with either RTA 408 or RTA 408 and IR. IR (5 Gy) was administered twice on days 1 and 8 and RTA 408 (17.5 mg/kg) was administered 1 day before and for 3 days after each IR in the combination group. RTA 408 administration (3 times weekly) was continued for further 4 weeks. Results represent mean ± SD of groups of 5 animals each. Tumor growth trajectories over time were compared between treatment and control groups, and among treatment groups. The insert shows representative images of tumors *in situ* at treatment start and 40 days after. Chemiluminescence was detected by IVIS bioimaging of PC3 cells constitutively expressing FLuc.

representing advanced, androgen-independent tumor stages (LNCaP/C4-2B, CWR22Rv1, DU145, and PC3). We observed robust tumor growth inhibition by RTA 408 of established xenografts (tumor size > 30 mm^3 when treatment commenced) of all four cell lines tested even in the absence of radiation. Tumor growth, as determined by caliper measurements, is shown in Fig. 3A and representative *in vivo* tumor images at different days after treatment in Supplementary Fig. S2. In marked contrast to the protective effects observed in normal tissues, RTA 408 did not radioprotect PC3 xenotransplants. Rather, when used in combination with radiation, RTA 408 amplified the antitumor effect of radiation alone ($P = 0.001$; Fig. 3B). *In vivo* imaging revealed complete tumor growth inhibition in animals that received both radiation and RTA 408 at 17.5 mg/kg (Fig. 3B, see insert) but not in mice treated with 5 mg/kg RTA 408 (not shown). RTA 408 induced high levels of intratumoral apoptosis as determined by detection of fragmented DNA (TUNEL), cleaved PARP, and the caspase-3 cleavage product of cytokeratin18 (Fig. 4A). The antibodies used to detect cleaved PARP and cytokeratin18 do not crossreact with mouse tissues indicating that RTA 408 induced apoptosis of human tumor cells *in situ*. RTA 408-dependent inhibition of PC3 xenografts was associated with significantly reduced proliferation as determined by Ki-67 staining (Fig. 4B).

RTA 408 decreases growth and survival of human prostate cancer cells *in vitro*

Next, we examined dose-dependent effects of RTA 408 on prostate cancer cells *in vitro*. Within 24 hours of exposure, RTA 408 (1 μmol/L) induced varying degrees of apoptosis in all four prostate cancer cell lines as determined by detection of cleaved caspase-3, cytokeratin18, and PARP-1 in both attached and, more prominently, in cells detached from substrate (Supplementary Fig. S3). In contrast, caspase-8 cleavage was only marginally detected in DU145 at the higher doses of RTA 408 (0.5–1 μmol/L) tested but not the other three cell lines. As determined by clonogenic survival assays, RTA 408 radiosensitized all four prostate cancer cell lines under investigation with the strongest effects observed in DU145 and LNCaP/C4-2B cells (Supplementary Fig. S4). As assessed by crystal violet staining and by WST assay, RTA 408 reduced viability of all four prostate cancer cell lines in a dose-dependent fashion (Fig. 5A). The IC_{50} for inhibition of *in vitro* growth and survival of these cell lines ranged from 250 to 750 nmol/L. Interestingly, RTA 408 also inhibited *in vitro* growth and survival of PrEC, the immortalized NHPr-E1 and BHPrE-1 prostate cells and, primary human epidermal keratinocytes (NHEK-1, -2, and -3; Fig. 5B). The IC_{50} as determined by crystal violet staining for the normal or premalignant cells was in the range of 125 to 250 nmol/L. Compromised cell viability was associated with substrate detachment of normal prostate epithelial cells and keratinocytes, as well as control PC3 cells (Supplementary Fig. S5). Collectively, these results highlight a broad spectrum of inhibitory effects of RTA 408 on benign and malignant prostate cells and on normal prostate epithelial cells and keratinocytes *in vitro*. The effects on normal epithelial cells *in vitro* are in marked contrast to tissue protection of normal epithelial tissues in irradiated mice.

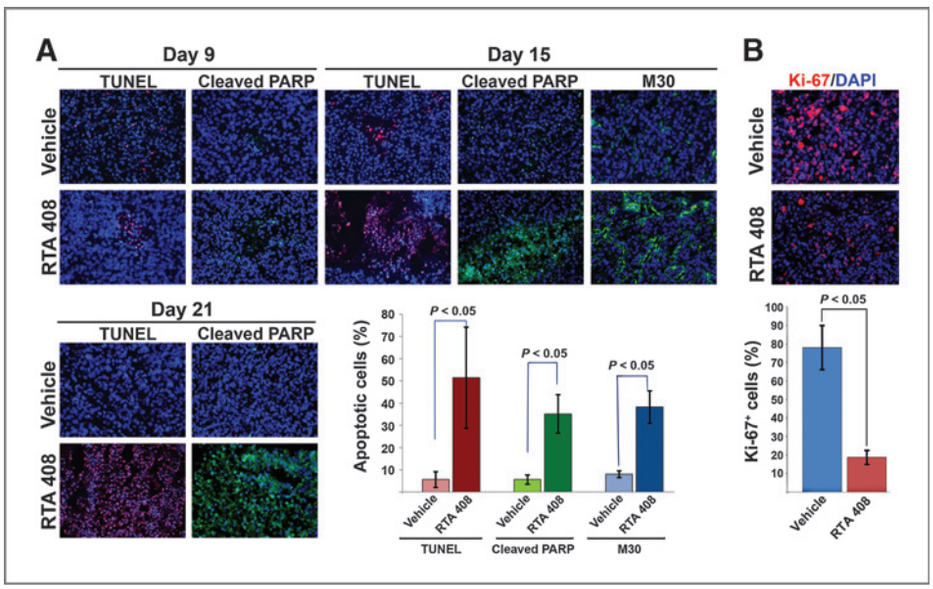

Figure 4. Effects of RTA 408 on apoptosis incidence and proliferation in PC3 prostate cancer xenografts treated with RTA 408. A, apoptosis incidence was determined by TUNEL and by immunohistochemical detection of cleaved PARP and cytokeratin 18 (M30) at different time intervals after treatment with RTA 408 commenced; scale bars = 100 μm. Quantitative analysis of the results obtained on day 15 of treatment was performed by averaging the number of positive cells in at least 6 different fields. Results are expressed as mean ± SD. Statistically significant ($P < 0.05$) differences were determined by Student *t* test. B, RTA 408-dependent inhibition of PC3 prostate cancer cell proliferation. Proliferating cells were detected by staining with Ki-67 antibody (red). Cell nuclei were counterstained with DAPI; scale bars = 100 μm. Tumors were harvested 15 days after treatment initiation.

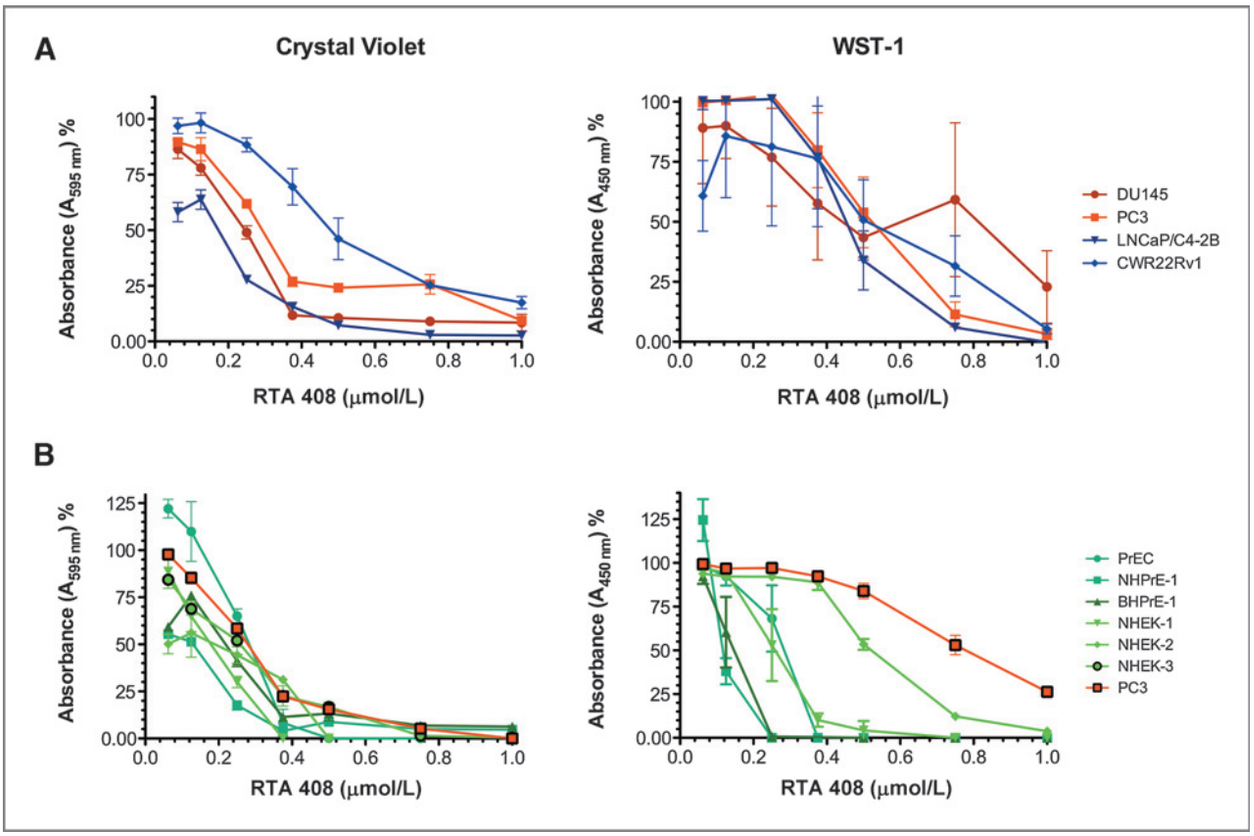

Figure 5. *In vitro* effects of RTA 408 on prostate cancer cell (A) and normal cell growth and survival (B). Loss of viability was determined by assessing the numbers of adherent cells using crystal violet stain or measuring metabolic activity (WST assay). Experiments were performed in triplicate and repeated two times. Results shown are mean ± SD of triplicates of a representative experiment. Results are presented as percentages of vehicle control. Analysis by using one-way ANOVA with Tukey posttest correction (GraphPad Prism) revealed significant differences between RTA 408– and vehicle-treated groups ($P < 0.05$ to $P < 0.001$).

Inhibition of NF-κB activity by RTA 408 *in vivo*

The selective antitumor activity of RTA 408 on prostate cancer cell lines *in vivo* raises the question which molecular target(s) are responsible for this effect. In prostate cancer, deregulated NF-κB signaling is associated with disease progression, contributes to expression of both prostate specific antigen (PSA; 21) and androgen receptor (22), and is prevalent in castrate-resistant and metastatic tumors (23–26). Conversely, disrupting NF-κB signaling by forced expression of a phosphorylation-deficient IκB radiosensitizes PC3 prostate cells *in vitro* (27). Other NF-κB inhibitors, including curcumin (28), parthenolide (29), and SN52 (30), similarly inhibit prostate cancer growth and survival. On the basis of this prior work, we used NF-κB-NLuc- and control CMV-Fluc -reporter constructs to measure NF-κB activity in transfected PC3 tumors *in vivo*, before and after treatment with RTA 408 and/or IR (Fig. 6A and B). As expected, radiation induced NF-κB activity in tumor tissue (Fig. 6, panel 4). In the posttreatment group, the ratio of NF-κB-NLuc- to CMV-Fluc activity in RTA 408-treated mice (Fig. 6, panel 6) was significantly lower compared with that observed in mice treated with vehicle alone (Fig. 6, panel 2). In addition, the ratio of NF-κB-NLuc- to CMV-Fluc activity in mice treated with RTA 408 and IR combined (Fig. 6, panel 8) was significantly lower compared with that observed in mice treated with IR alone (Fig. 6, panel 4). Hence, at tumor growth–inhibitory concentrations, RTA 408 effectively inhibited transcription of an NF-κB–responsive reporter construct in PC3 cells *in vivo*.

These observations extend and confirm previous reports describing *in vitro* growth inhibition of human prostate cancer cells by CDDO variants. Specifically, Deeb and colleagues described proapoptotic effects of CDDO, CDDO-methyl(ME), and CDDO-imidazole(IM) in cultured human LNCaP, PC3, and DU145 and murine TRAMPC-1 prostate cancer cells *in vitro* (31, 32). Furthermore, Gao and colleagues described CDDO-dependent chemoprevention of prostate cancer development in transgenic TRAMP mice in which the SV40 T antigen is expressed by prostate epithelial cells (33). Tumor growth inhibition by CDDO derivatives extends to other tumor types ranging from leukemias (34–37) to solid malignancies (38–42). A common denominator of these tumor types is deregulated NF-κB activity, which is effectively inhibited by RTA 408 not only *in vitro* but also *in vivo*. It remains

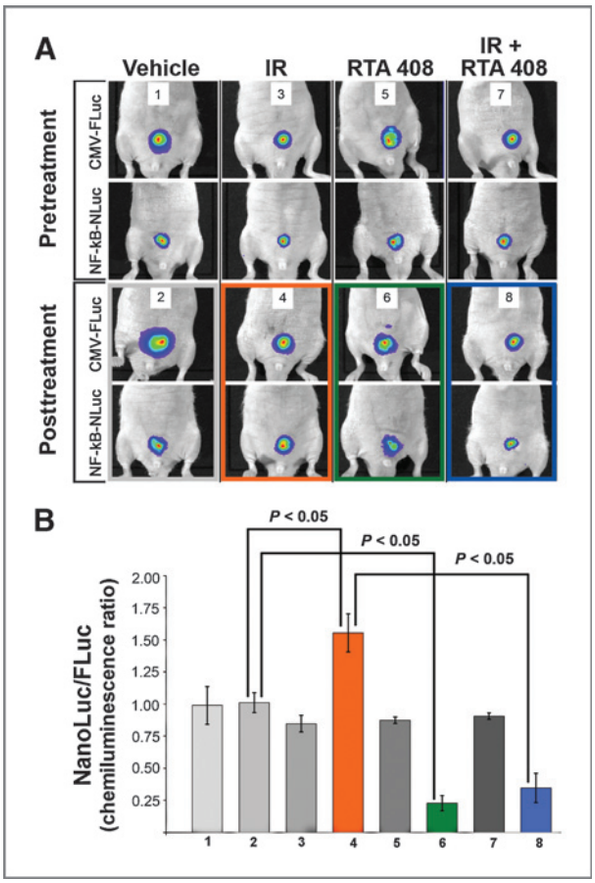

Figure 6. *In vivo* imaging of NF-κB reporter activity in PC3 xenografts treated with either IR, or RTA 408, or a combination of IR and RTA 408. A, representative images of mice showing expression of FLuc under control of a CMV promoter and corresponding images showing activity of an NF-κB–responsive promoter driving NanoLuc (NLuc) expression are shown. Pretreatment images were acquired 2 days before treatment with either RTA 408 or IR (panels 1, 3, 5, and 7). Posttreatment images were acquired from the same mice either untreated or after short-term (1 hour) treatment with RTA 408 (17.5 mg/kg) or after IR (5 Gy) or RTA 408 (17.5 mg/mL; 2 days) and IR (5 Gy) as indicated (panels 2, 4, 6, 8). Images in the posttreatment group were acquired 1 hour after IR exposure. B, quantitative representation of NF-κB activity expressed as the ratio of NanoLuc to firefly luciferase ($n = 2$/group). Labeling of the x-axis refers to treatment groups as shown in A. Results shown are mean ± SD of duplicate mice in each group. This experiment was repeated with comparable results.

to be determined whether inhibition of survival pathways beyond NF-κB plays a role in prostate cancer inhibition by RTA 408. For example, the Akt/mTOR pathway is also reportedly inhibited by CDDO-ME in prostate cancer cells (43).

The mechanistic basis for the dual and opposite effects of RTA 408 on normal and a broad range of malignant tissues remains to be investigated further. Of particular relevance to cytoprotection, CDDO covalently attaches to KEAP1, disrupts KEAP1/Nrf2 interaction, and triggers Nrf2-dependent transcription of a host of genes encoding antioxidant enzymes (16). Nrf-2 activation by the CDDO derivatives CDDO-ethylamide (EA) and CDDO-ME has been proposed to improve survival of irradiated mice (44). We observed that topical application of RTA 408 markedly reduced radiation dermatitis in mice associated with significant increases in Nrf2 target genes and significant decreases in NF-κB target genes (45). Interestingly, radiation protection of normal prostate epithelial cells contrasted by growth inhibition of prostate cancer cells *in vivo* has been very recently described for dimethylamineparthenolide (DMAPT; ref. 46). DMAPT and its parent compound parthenolide alkylate reactive cysteines on multiple protein targets, including KEAP1, inhibit canonical NF-κB signaling by interacting with IκB and the NFκBp65 subunit (47–49). In contrast to RTA 408, parthenolide or DMAPT reportedly did not inhibit cultured normal or immortalized prostate cells to the same extent as their malignant counterparts and this difference has been attributed to differential effects of DMAPT on KEAP1-dependent oxidation status in normal and malignant cells (46). This difference between RTA 408 and DMAPT suggests that tissue protection by RTA 408 as seen *in vivo* is not primarily due to cell-autonomous effects but likely depends on environmental factors provided by the tissue context *in vivo*. A precedent for "contextual" antitumor effects of CDDO-ME has been established previously (50). Specifically, CDDO-ME inhibited myeloid-derived suppressor cells in the tumor microenvironment associated with improved immune responses. Regardless of the relative contribution of cell-intrinsic or "environmental" antitumor mechanisms, the results obtained for DMAPT (46) and RTA 408 (this study) validate the concept of selective radiosensitization of tumor cell tissues by thiol-reactive compounds (5).

Disclosure of Potential Conflicts of Interest

K. Ward is VP, Early Development and has ownership interest (including patents) in Reata Pharmaceuticals. U. Rodeck reports receiving a commercial research grant from REATA Pharmaceuticals. No potential conflicts of interest were disclosed by the other authors.

Authors' Contributions

Conception and design: K. Ward, A.P. Dicker, U. Rodeck
Development of methodology: V. Alexeev, A. Linnenbach
Acquisition of data (provided animals, acquired and managed patients, provided facilities, etc.): V. Alexeev, E. Lash, A. Bitterman, A. Linnenbach, U. Rodeck
Analysis and interpretation of data (e.g., statistical analysis, biostatistics, computational analysis): V. Alexeev, L. Corsini, A. Bitterman, A.P. Dicker, A. Linnenbach
Writing, review, and/or revision of the manuscript: V. Alexeev, K. Ward, A.P. Dicker, A. Linnenbach, U. Rodeck
Administrative, technical, or material support (i.e., reporting or organizing data, constructing databases): E. Lash, A. Aguillard, L. Corsini, A.P. Dicker, U. Rodeck
Study supervision: U. Rodeck

Acknowledgments

The authors thank Phyllis Wachsberger (Thomas Jefferson University, Philadelphia, PA) for advice on performing clonogenic assays, Simon Hayward (Vanderbilt University, Nashville, TN) for providing immortalized prostate cells and Marja Nevalainen (Thomas Jefferson University, Philadelphia, PA) for providing prostate cancer cells.

Grant Support

This work was supported by DoD grant W81XWH-12-1-0477 and a pilot project under NIH grant U19A1091175. Additional support was provided by the Prostate Cancer Foundation and by REATA Pharmaceuticals.

The costs of publication of this article were defrayed in part by the payment of page charges. This article must therefore be hereby marked *advertisement* in accordance with 18 U.S.C. Section 1734 solely to indicate this fact.

Received April 24, 2014; revised September 2, 2014; accepted September 16, 2014; published OnlineFirst xx xx, xxxx.

References

1. Kountouras J, Zavos C. Recent advances in the management of radiation colitis. World J Gastroenterol 2008;14:7289–301.
2. Souhami L, Bae K, Pilepich M, Sandler H. Impact of the duration of adjuvant hormonal therapy in patients with locally advanced prostate cancer treated with radiotherapy: a secondary analysis of RTOG 85–31. J Clin Oncol 2009;27:2137–43.
3. Simone NL, Menard C, Soule BP, Albert PS, Guion P, Smith S, et al. Intrarectal amifostine during external beam radiation therapy for prostate cancer produces significant improvements in Quality of Life measured by EPIC score. Int J Radiat Oncol Biol Phys 2008;70:90–5.
4. Spitz DRD, Hauer-Jensen M. Ionizing radiation-induced responses: where free radical chemistry meets redox biology and medicine. Antioxid Redox Signal 2014;20:1407–9.
5. Deorukhkar A, Krishnan S. Targeting inflammatory pathways for tumor radiosensitization. Biochem Pharmacol 2010;80:1904–14.
6. Daroczi B, Kari G, Ren Q, Dicker AP, Rodeck U. Nuclear factor kappaB inhibitors alleviate and the proteasome inhibitor PS-341 exacerbates radiation toxicity in zebrafish embryos. Mol Cancer Ther 2009;8:2625–34.
7. Thotala DK, Hallahan DE, Yazlovitskaya EM. Inhibition of glycogen synthase kinase 3 beta attenuates neurocognitive dysfunction resulting from cranial irradiation. Cancer Res 2008;68:5859–68.
8. Thotala DK, Geng L, Dickey AK, Hallahan DE, Yazlovitskaya EM. A new class of molecular targeted radioprotectors: GSK-3beta inhibitors. Int J Radiat Oncol Biol Phys 2010;76:557–65.
9. Jacobs KM, Bhave SR, Ferraro DJ, Jaboin JJ, Hallahan DE, Thotala D. GSK-3beta: A Bifunctional Role in Cell Death Pathways. Int J Cell Biol 2012;2012:930710.
10. Hoeflich KP, Luo J, Rubie EA, Tsao MS, Jin O, Woodgett JR. Requirement for glycogen synthase kinase-3beta in cell survival and NF-kappaB activation. Nature 2000;406:86–90.
11. Cremer TJ, Shah P, Cormet-Boyaka E, Valvano MA, Butchar JP, Tridandapani S. Akt-mediated proinflammatory response of mononuclear phagocytes infected with Burkholderia cenocepacia occurs by a novel GSK3beta-dependent, IkappaB kinase-independent mechanism. J Immunol 2011;187:635–43.
12. Hall EJ, Giaccia AJ. Cell survival curves. Radiobiology for the radiologist. Philadelphia, PA: Lippincott Williams & Wilkins; 2006. p. 30–46.
13. Epperly M, Jin S, Nie S, Cao S, Zhang X, Franicola D, et al. Ethyl pyruvate, a potentially effective mitigator of damage after total-body irradiation. Radiat Res 2007;168:552–9.
14. Daroczi B, Kari G, McAleer MF, Wolf JC, Rodeck U, Dicker AP. *In vivo* radioprotection by the fullerene nanoparticle DF-1 as assessed in a zebrafish model. Clin Cancer Res 2006;12:7086–91.
15. Han Y, Englert JA, Yang R, Delude RL, Fink MP. Ethyl pyruvate inhibits nuclear factor-kappaB-dependent signaling by directly targeting p65. J Pharmacol Exp Ther 2005;312:1097–105.
16. Ahmad R, Raina D, Meyer C, Kharbanda S, Kufe D. Triterpenoid CDDO-Me blocks the NF-kappaB pathway by direct inhibition of IKKbeta on Cys-179. J Biol Chem 2006;281:35764–9.
17. Liby K, Hock T, Yore MM, Suh N, Place AE, Risingsong R, et al. The synthetic triterpenoids, CDDO and CDDO-imidazolide, are potent inducers of heme oxygenase-1 and Nrf2/ARE signaling. Cancer Res 2005;65:4789–98.
18. Coghlan MP, Culbert AA, Cross DA, Corcoran SL, Yates JW, Pearce NJ, et al. Selective small molecule inhibitors of glycogen synthase kinase-3 modulate glycogen metabolism and gene transcription. Chem Biol 2000;7:793–803.
19. Zhang F, Phiel CJ, Spece L, Gurvich N, Klein PS. Inhibitory phosphorylation of glycogen synthase kinase-3 (GSK-3) in response to lithium. Evidence for autoregulation of GSK-3. J Biol Chem 2003;278:33067–77.
20. Saha S, Bhanja P, Liu L, Alfieri AA, Yu D, Kandimalla ER, et al. TLR9 agonist protects mice from radiation-induced gastrointestinal syndrome. PLoS ONE 2012;7:e29357.
21. Chen CD, Sawyers CL. NF-kappa B activates prostate-specific antigen expression and is upregulated in androgen-independent prostate cancer. Mol Cell Biol 2002;22:2862–70.
22. Zhang L, Altuwaijri S, Deng F, Chen L, Lal P, Bhanot UK, et al. NF-kappaB regulates androgen receptor expression and prostate cancer growth. Am J Pathol 2009;175:489–99.
23. McCall P, Bennett L, Ahmad I, Mackenzie LM, Forbes IW, Leung HY, et al. NFkappaB signalling is upregulated in a subset of castrate-resistant prostate cancer patients and correlates with disease progression. Br J Cancer 2012;107:1554–63.
24. Siddiqui IA, Shukla Y, Adhami VM, Sarfaraz S, Asim M, Hafeez BB, et al. Suppression of NFkappaB and its regulated gene products by oral administration of green tea polyphenols in an autochthonous mouse prostate cancer model. Pharm Res 2008;25:2135–42.
25. Andela VB, Gordon AH, Zotalis G, Rosier RN, Goater JJ, Lewis GD, et al. NFkappaB: a pivotal transcription factor in prostate cancer metastasis to bone. Clin Orthop Relat Res 2003:S75–85.
26. Jin R, Sterling JA, Edwards JR, DeGraff DJ, Lee C, Park SI, et al. Activation of NF-kappa B signaling promotes growth of prostate cancer cells in bone. PLoS ONE 2013;8:e60983.
27. Pajonk F, Pajonk K, McBride WH. Inhibition of NF-kappaB, clonogenicity, and radiosensitivity of human cancer cells. J Natl Cancer Inst 1999;91:1956–60.
28. Chendil D, Ranga RS, Meigooni D, Sathishkumar S, Ahmed MM. Curcumin confers radiosensitizing effect in prostate cancer cell line PC-3. Oncogene 2004;23:1599–607.
29. Sun Y, St Clair DK, Fang F, Warren GW, Rangnekar VM, Crooks PA, et al. The radiosensitization effect of parthenolide in prostate cancer cells is mediated by nuclear factor-kappaB inhibition and enhanced by the presence of PTEN. Mol Cancer Ther 2007;6:2477–86.
30. Xu Y, Fang F, St Clair DK, Sompol P, Josson S, St Clair WH. SN52, a novel nuclear factor-kappaB inhibitor, blocks nuclear import of RelB:p52 dimer and sensitizes prostate cancer cells to ionizing radiation. Mol Cancer Ther 2008;7:2367–76.
31. Deeb D, Gao X, Dulchavsky SA, Gautam SC. CDDO-me induces apoptosis and inhibits Akt, mTOR and NF-kappaB signaling proteins in prostate cancer cells. Anticancer Res 2007;27:3035–44.
32. Deeb D, Gao X, Dulchavsky SA, Gautam SC. CDDO-Me inhibits proliferation, induces apoptosis, down-regulates Akt, mTOR, NF-kappaB and NF-kappaB-regulated antiapoptotic and proangiogenic proteins in TRAMP prostate cancer cells. J Exp Ther Oncol 2008;7:31–9.
33. Gao X, Deeb D, Liu Y, Arbab AS, Divine GW, Dulchavsky SA, et al. Prevention of prostate cancer with oleanane synthetic triterpenoid CDDO-Me in the TRAMP mouse model of prostate cancer. Cancers 2011;3:3353–69.
34. Shishodia S, Sethi G, Konopleva M, Andreeff M, Aggarwal BB. A synthetic triterpenoid, CDDO-Me, inhibits IkappaBalpha kinase and enhances apoptosis induced by TNF and chemotherapeutic agents through down-regulation of expression of nuclear factor kappaB-regulated gene products in human leukemic cells. Clin Cancer Res 2006;12:1828–38.
35. Samudio I, Kurinna S, Ruvolo P, Korchin B, Kantarjian H, Beran M, et al. Inhibition of mitochondrial metabolism by methyl-2-cyano-3,12-dioxooleana-1,9-diene-28-oate induces apoptotic or autophagic cell

death in chronic myeloid leukemia cells. Mol Cancer Ther 2008; 7:1130–9.
36. Stadheim TA, Suh N, Ganju N, Sporn MB, Eastman A. The novel triterpenoid 2-cyano-3,12-dioxooleana-1,9-dien-28-oic acid (CDDO) potently enhances apoptosis induced by tumor necrosis factor in human leukemia cells. J Biol Chem 2002;277:16448–55.
37. Pedersen IM, Kitada S, Schimmer A, Kim Y, Zapata JM, Charboneau L, et al. The triterpenoid CDDO induces apoptosis in refractory CLL B cells. Blood 2002;100:2965–72.
38. Qin Y, Deng W, Ekmekcioglu S, Grimm EA. Identification of unique sensitizing targets for anti-inflammatory CDDO-Me in metastatic melanoma by a large-scale synthetic lethal RNAi screening. Pigment Cell Melanoma Res 2013;26:97–112.
39. Konopleva M, Zhang W, Shi YX, McQueen T, Tsao T, Abdelrahim M, et al. Synthetic triterpenoid 2-cyano-3,12-dioxooleana-1,9-dien-28-oic acid induces growth arrest in HER2-overexpressing breast cancer cells. Mol Cancer Ther 2006;5:317–28.
40. Duan Z, Ames RY, Ryan M, Hornicek FJ, Mankin H, Seiden MV. CDDO-Me, a synthetic triterpenoid, inhibits expression of IL-6 and Stat3 phosphorylation in multi-drug resistant ovarian cancer cells. Cancer Chemother Pharmacol 2009;63:681–9.
41. Gao X, Deeb D, Liu P, Liu Y, Arbab-Ali S, Dulchavsky SA, et al. Role of reactive oxygen species (ROS) in CDDO-Me-mediated growth inhibition and apoptosis in colorectal cancer cells. J Exp Ther Oncol 2011;9:119–27.
42. Zou W, Chen S, Liu X, Yue P, Sporn MB, Khuri FR, et al. c-FLIP downregulation contributes to apoptosis induction by the novel synthetic triterpenoid methyl-2-cyano-3, 12-dioxooleana-1, 9-dien-28-oate (CDDO-Me) in human lung cancer cells. Cancer Biol Ther 2007;6:1614–20.
43. Deeb D, Gao X, Jiang H, Janic B, Arbab AS, Rojanasakul Y, et al. Oleanane triterpenoid CDDO-Me inhibits growth and induces apoptosis in prostate cancer cells through a ROS-dependent mechanism. Biochem Pharmacol 2010;79:350–60.
44. Kim SB, Pandita RK, Eskiocak U, Ly P, Kaisani A, Kumar R, et al. Targeting of Nrf2 induces DNA damage signaling and protects colonic epithelial cells from ionizing radiation. Proc Natl Acad Sci U S A 2012;109:E2949–55.
45. Reisman SA, Lee C-Y, Meyer CJ, Proksch JW, Sonis ST, Ward KW. Topical application of the synthetic triterpenoid RTA 408 protects mice from radiation-induced dermatitis. Radiat Res 2014;181: 512–20.
46. Xu Y, Fang F, Miriyala S, Crooks PA, Oberley TD, Chaiswing L, et al. KEAP1 is a redox sensitive target that arbitrates the opposing radiosensitive effects of parthenolide in normal and cancer cells. Cancer Res 2013;73:4406–17.
47. Garcia-Pineres AJ, Castro V, Mora G, Schmidt TJ, Strunck E, Pahl HL, et al. Cysteine 38 in p65/NF-kappaB plays a crucial role in DNA binding inhibition by sesquiterpene lactones. J Biol Chem 2001;276:39713–20.
48. Kwok BH, Koh B, Ndubuisi MI, Elofsson M, Crews CM. The anti-inflammatory natural product parthenolide from the medicinal herb Feverfew directly binds to and inhibits IkappaB kinase. Chem Biol 2001;8:759–66.
49. Hehner SP, Hofmann TG, Droge W, Schmitz ML. The antiinflammatory sesquiterpene lactone parthenolide inhibits NF-kappa B by targeting the I kappa B kinase complex. J Immunol 1999;163:5617–23.
50. Nagaraj S, Youn JI, Weber H, Iclozan C, Lu L, Cotter MJ, et al. Anti-inflammatory triterpenoid blocks immune suppressive function of MDSCs and improves immune response in cancer. Clin Cancer Res 2010;16:1812–23.

AUTHOR QUERIES

AUTHOR PLEASE ANSWER ALL QUERIES

Q1: Page: 1: AU: Per journal style, genes, alleles, loci, and oncogenes are italicized; proteins are roman. Please check throughout to see that the words are styled correctly. AACR journals have developed explicit instructions about reporting results from experiments involving the use of animal models as well as the use of approved gene and protein nomenclature at their first mention in the manuscript. Please review the instructions at http://www.aacrjournals.org/site/InstrAuthors/ifora.xhtml#genenomen to ensure that your article is in compliance. If your article is not in compliance, please make the appropriate changes in your proof.

Q2: Page: 1: Author: The phone and fax details of the corresponding author are same. Please verify.

Q3: Page: 1: Author: Please verify the drug names and their dosages used in the text.

Q4: Page: 1: Author: Units of measurement have been changed here and elsewhere in the text from "M" to "mol/L," and related units, such as "mmol/L" and "μmol/L," in figures, legends, and tables in accordance with journal style, derived from the Council of Science Editors Manual for Authors, Editors, and Publishers and the Système international d'unités. Please note if these changes are not acceptable or appropriate in this instance.

Q5: Page: 3: Author: Please confirm the quality/labeling of all images included within this article. Thank you.

Q6: Page: 5: AU: Please verify the presentation of "mean $\pm$ SD" in figure legends 3, 5 and 6.

Q7: Page: 8: Author: Please verify the changes made in the sentence "DMAPT and its . . . NFκBp65 subunit" for correctness.

Q8: Page: 8: AU/PE: The conflict-of-interest disclosure statement that appears in the proof incorporates the information from forms completed and signed off on by each individual author. No factual changes can be made to disclosure information at the proof stage. However, typographical errors or misspelling of author names should be noted on the proof and will be corrected before publication. Please note if any such errors need to be corrected. Is the disclosure statement correct?

Q9: Page: 8: Author: The contribution(s) of each author are listed in the proof under the heading "Authors' Contributions." These contributions are derived from forms completed and signed off on by each individual author. As the corresponding author, you are permitted to make changes to your own contributions. However, because all authors submit their contributions individually, you are not permitted to make changes in the contributions listed for any other authors. If you feel strongly that an error is being made, then you may ask the author or authors in question to contact us about making the changes. Please note, however, that the manuscript would be held from further processing until this issue is resolved.

Q10: Page: 9: Author: Please note that Ref. 4 has been updated as per PubMed. Please verify.

AU: Below is a summary of the name segmentation for the authors according to our records. The First Name and the Surname data will be provided to PubMed when the article is indexed for searching. Please check each name carefully and verify that the First Name and Surname are correct. If a name is not segmented correctly, please write the correct First Name and Surname on this page and return it with your proofs. If no changes are made to this list, we will assume that the names are segmented correctly, and the names will be indexed as is by PubMed and other indexing services.

First Name	**Surname**
Vitali	Alexeev
Elizabeth	Lash
April	Aguillard
Laura	Corsini
Avi	Bitterman
Keith	Ward
Adam P.	Dicker
Alban	Linnenbach
Ulrich	Rodeck

The triterpenoid RTA 408 is a robust mitigator of hematopoietic acute radiation syndrome in mice

Devorah C. Goldman[1], Vitali Alexeev[2], Elizabeth Lash[2], Chandan Guha[3], Ulrich Rodeck[2]* and William H. Fleming[1*‡]

[1]Department of Pediatrics, Oregon Stem Cell Center, Knight Cancer Institute, Oregon Health & Science University, Portland, OR 97239, [2]Departments of Dermatology and Radiation Oncology, Thomas Jefferson University, Philadelphia, PA 19107 and [3]Department of Radiation Oncology, Albert Einstein College of Medicine, The Montefiore Medical Center, Bronx, NY 10467.

* These authors contributed equally to this manuscript

Corresponding authors:

William H. Fleming
Ulrich Rodeck

Oregon Health & Science University
Thomas Jefferson University

3181 S.W. Sam Jackson Park Road
233 S 10th Street

Mail Code L321
BLSB409

Portland, OR 97239
Philadelphia, PA 19130

Email: flemingw@ohsu.edu
Email: ulrich.rodeck@jefferson.edu
Telephone: 503 494 2772
Telephone: 215 503 5622
FAX: 503 418 5044
FAX: 215 503 5788

Running Title: RTA 408 mitigates hematopoietic syndrome

Goldman DC, Alexeev V, Guha C, Rodeck U and Fleming WH**.** The triterpenoid RTA 408 is a robust mitigator of radiation-induced hematopoietic syndrome in mice. *Radiat. Res*.

Abstract

Bone marrow suppression due to ionizing radiation is a significant clinical problem in radiation therapy and following non-medical radiation exposure. Currently, no small molecule agents that can enhance hematopoietic regeneration following radiation exposure are available. Here, we report the effective mitigation of acute hematopoietic radiation syndrome in mice by the synthetic triterpenoid, RTA 408. The administration of a brief course of RTA 408 treatment beginning 24 h after bone marrow lethal doses of radiation significantly increased overall survival. Importantly, treatment with RTA 408 led to the full recovery of steady state hematopoiesis with normalization of the frequency of hematopoietic stem and progenitor cells. Moreover, hematopoietic stem cells from RTA 408-mitigated mice showed lineage-balanced, long-term, multilineage potential in serial transplantation assays, indicative of their normal self-renewal activity. The potency of RTA 408 in mitigating radiation-induced bone marrow suppression makes it an attractive candidate for potential clinical use in treating both therapy-related and unanticipated radiation exposure.

Introduction

Tissue damage due to intentional or accidental radiation exposure is a pervasive threat. Dispersal of radioactive materials leading to whole body exposure may occur as a consequence of nuclear reactor incidents (e.g. Fukushima) or following detonation of explosive devices laced with radioactive materials (e.g. 'dirty bomb'). One of the most highly proliferative tissues in the body, the hematopoietic system, is also the most sensitive to the effects of ionizing radiation. At relatively low doses of exposure, radiation-induced damage to hematopoietic cells can cause bone marrow failure, leading to anemia, infection and hemorrhage [1,2]. Even exposure to non-lethal doses of radiation causes significant injury to hematopoietic stem cells (HSCs), and causes their depletion, increased differentiation and impaired self-renewal activity [3]. To be useful in the setting of unanticipated radiation exposure, therapeutic agents must effectively mitigate radiation damage when administered after the exposure has occurred. To date, no small molecule pharmacological drugs are approved to treat radiation-induced hematopoietic syndrome either in the radioprotection or mitigation setting [4].

Triterpenoids bind to specific cysteine residues on target proteins [5] and elicit both cytoprotective [6] and anti-inflammatory activities [7,8]. While it is unresolved which molecular targets of triterpenoids impart cytoprotection, these compounds induce antioxidant enzymes in an Nrf2-dependent fashion [9,10] and inhibit canonical NF-κB signaling [11]. Earlier work demonstrated that triterpenoids protect zebrafish embryos against the lethal effects of ionizing radiation [12]. More recently, a triterpenoid (CDDO-Me) administered 24 hours after radiation exposure was shown to improve the survival of mice exposed to lethal, myelosuppressive doses of total body radiation (TBI) [13]. Although CDDO-Me advanced to phase III clinical trials to treat diabetes-associated chronic kidney disease, further development of this compound was stopped due to adverse events related to fluid overload in a subset of these renal failure patients [14].

In this report, we focus on the mitigation of the hematopoietic acute radiation syndrome by a triterpenoid (RTA 408) that is currently in clinical development for oncological applications. Recent work demonstrated that RTA 408 protects the skin [15] and gastrointestinal mucosa (Alexeev et al., in revision) of mice against radiation damage. These findings encouraged us to investigate whether RTA 408 also can

increase hematopoietic recovery from radiation damage, and can be used in the mitigation setting, i.e. when administered 24 h after radiation exposure. We observed that RTA 408 was a highly effective mitigator of hematopoietic syndrome in mice as demonstrated by effective recovery of hematopoiesis after administration of lethal, myeloablative doses of whole body radiation. In addition, treatment with RTA 408 restored normal hematopoietic stem and progenitor cell frequency and HSC-self renewal activity.

Materials and Methods

Radiation exposure and mitigator treatment

RTA 408 was provided by REATA Pharmaceuticals, Inc. and DMSO stock solutions prepared within 1 h before injection. RTA 408 (17.5 mg/kg) or vehicle control (DMSO) were administered intraperitoneally (i.p.) at 24, 48 and 72 h after irradiation. Whole body ionizing radiation (IR) was administered at doses ranging from 7 to 8 Gy using a 250-kVp X-ray machine (PanTak, East Haven, CT) with 50-cm source-to-skin distance and a 2-mm copper filter. The dose rate was approximately 1.4 Gy/min.

Mice

For initial irradiation experiments, C57Bl/6 mice (6-8 weeks old) were used. For transplantation studies, 8-12 week old C57Bl/6 CD45.1 or C57Bl/6 CD45.1/CD45.2 hybrid host mice were used as recipients and as carrier cell donors. Mice were kept in pathogen-free conditions and handled in accordance with the requirements of the Guideline for Animal Experiments and after approval of the experimental protocols by the Institutional Animal Care and Use Committees of Thomas Jefferson University and OHSU.

Complete blood counts and bone marrow analysis

Peripheral blood was collected into tubes containing EDTA tripotassium salt and assayed using a Hemavet 950 FS hematology analyzer. Dissected femurs were flushed with Hank's Balanced Salt Solution containing 10mM HEPES and 3% fetal bovine serum and passed through a 70 micron cell strainer. Nucleated cell counts were obtained using Turk's solution and a hemocytometer.

Colony forming unit (CFU) assays

Bone marrow cells ($2x10^4$) were plated in duplicate or triplicate in 35mm dishes in mouse methylcellulose complete medium (HSC007, R&D systems). Colonies were scored 7-10 days after plating following the manufacturer's instructions.

Transplantation studies

Prior to transplant, all recipient mice were maintained for at least one week on acidified water. Recipient mice received 7.5 Gy in a single fraction using an RS2000 Xray irradiator (Rad Source, Alpharetta, Georgia) with a dose rate of ~1.36 Gy/min. Primary cell recipients received $2x10^6$ donor cells together with $1x10^5$ carrier bone marrow. For serial transplantation experiments, secondary recipient mice received $2x10^6$ unfractionated bone marrow isolated from primary recipients. Immediately following irradiation, cells were transplanted into anesthetized animals via retroorbital injection. Recipient mice were maintained on water containing antibiotics for 4 weeks following transplant, as previously described [16].

Flow cytometry

Red-cell depleted peripheral blood was prepared as previously described [17]. Live cells were stained with antibodies, washed and then analyzed using a Canto or LSR II (BD). Dead cells were excluded with propidium iodine and doublets were excluded using FSC-A, FSC-H and trigger pulse width parameters. Data were analyzed with FlowJo software (Tree Star, Inc, Philomath, OR, USA). Antibodies (and clones) used in this study include: Mac1 (M1/70), Gr1 (RB6-8C5), B220 (RA3-6B2), CD3 (145-2C11), and c-kit (2B8) from eBioscience (San Diego, CA, USA); CD4 (H29.19), CD5 (53-7.3), CD8 (53.6.7) from BD Pharmingen; TER119, Sca1 (D7), CD150 (TC15-12F12.2), from Biolegend (San Diego, CA, USA). For LSK cell analysis, the lineage panel included B220, CD3, CD4, CD5, CD8, Mac1, Gr1 and Ter119.

Results

RTA 408 enhances the survival of lethally irradiated mice

To determine whether RTA 408 is an effective mitigator of hematopoietic acute radiation syndrome following bone marrow-lethal doses of total body irradiation (TBI), mice were administered 3 daily injections of 17.5 mg/kg RTA 408 beginning 24 hours following TBI (Figure 1 A). Remarkably, treatment with RTA 408 resulted in the 35 day survival of 100% of 7Gy ($LD_{40/35}$) TBI mice (Figure 1B, $P<0.05$) and 60% of 7.5 Gy ($LD_{100/13}$) TBI mice (Figure 1C, $P<0.0001$). Although 40% of mice exposed to 8 Gy ($LD_{100/10}$) TBI survived following RTA 408 treatment, these results did not reach statistical significance (Figure 1D).

Full hematologic recovery in irradiated mice treated with RTA 408.

To begin to assess the recovery of hematopoiesis, complete blood counts (CBCs) were obtained at 2 weeks and again at 11 weeks following RTA 408 treatment. As anticipated, both neutrophils and lymphocytes were markedly reduced at 2 weeks; however, the hemoglobin remained above 8 g/dL, a level consistent with survival from a bone marrow lethal dose of radiation. By 11 weeks after radiation exposure, most parameters had returned to normal in the RTA 408 treated mice (Figure 2A). Circulating neutrophils were increased in RTA 408-treated mice relative to non-irradiated age matched control mice. This result was not surprising as the percentage of neutrophils in the blood is typically increased in mice following either bone marrow or hematopoietic stem cell transplant. This myeloid bias may be further amplified as the triterpenoid derivative CDDO-Me is known to promote myelopoiesis in mice [18]. In $LD_{(50/30)}$-$LD_{(70/30)}$ TBI mice that survive radiation injury without any intervention, BM cellularity typically remains significantly decreased throughout life [19]. However, when we assessed BM in RTA 408-treated 7.5 Gy TBI mice 14 weeks after radiation exposure, BM cellularity was not reduced in the TBI+RTA 408 mice (Figure 2B). Together, these findings of the complete restoration of circulating hematopoietic cells and normal BM cellularity in 7.5 Gy TBI mice indicate that RTA 408 is a potent mitigator of hematopoietic syndrome.

RTA 408 restores normal hematopoietic stem and progenitor cell frequency in lethally irradiated mice

Acute radiation exposure causes long-term damage to both hematopoietic stem and progenitor cells, resulting in their decreased frequency and a substantive loss of functional activity [3,19-21]. To more fully assess the efficacy of RTA 408 in restoring hematopoietic stem and progenitor cell frequency following lethal irradiation, BM from RTA 408-treated mice was analyzed 14 weeks following 7.5 Gy TBI (Figure 1A). BM from age-matched, non-irradiated mice was used for comparison as none of the vehicle-treated 7.5 Gy TBI mice survived (Figure 1C). Flow cytometric analysis (Figure 3A) revealed that mice exposed to TBI and treated with RTA 408 had comparable frequencies of phenotypic progenitor cells including $Linage^{-}(Lin^{-})$ $ckit^{+}$ cells and $Lin^{-}Sca1^{-}c\text{-}kit^{+}$ ($LS^{neg}K$) myeloerythroid committed progenitors. Similarly, a normal frequency of $Lin^{-}Sca1^{+}c\text{-}kit^{+}$ (LSK) cells, a subpopulation highly enriched for hematopoietic stem cells and multipotent progenitor cells, was observed in RTA 408-mitigated mice (Figure 3B). Hematopoietic progenitor cell function in RTA 408-mitigated 7.5 Gy TBI mice was further assessed by measuring BM colony forming unit (CFU) activity on a per cell basis in cytokine- supplemented methylcellulose. Both the total frequency and the individual subsets of myeloerythroid colonies formed by RTA 408-mitigated BM were indistinguishable from those formed by non-TBI control BM (Figure 3C), indicating no loss of progenitor activity in the RTA 408-mitigated BM. Together, these data demonstrate that RTA 408 treatment of 7.5 Gy mice exposed to TBI restored both phenotypic and functional hematopoietic progenitors to normal levels.

To assess phenotypic HSCs in RTA 408-mitigated 7.5 Gy TBI mice, the frequency of $CD150^{+}$LSK cells, a population that is highly enriched for functional stem cells [22], was determined by flow cytometry. Both the absolute number and frequency of $CD150^{+}$LSK cells in RTA 408 treated TBI mice was the same as that in non-TBI controls (Figure 3D). It has previously been shown that radiation injury causes a long-term phenotypic skewing of hematopoietic stem cells, reflected by a higher proportion of $CD150^{+}$ cells within the LSK cell subset [19,21]. However, the proportion of $CD150^{+}$ cells in the LSK cell population of RTA 408-mitigated TBI mice was the same as that observed in age-matched non-TBI mice (Figure 3E). Thus, RTA 408 treatment 24 hours post-TBI both effectively mitigates the radiation-induced loss of phenotypic HSCs.

RTA 408 restores functional HSCs in lethally irradiated mice.

Transplantation assays were performed to assess the long-term functional status of HSCs in RTA 408-rescued mice. For these experiments, BM from individual RTA 408 treated mice has harvested 3.5 months post TBI was co-transplanted with a limiting dose of carrier BM into CD45 congenic, lethally irradiated recipients (Figure 4A). Donor cell engraftment was monitored in the peripheral blood over time. Radiation exposure not only limits HSC self-renewal, it also causes their long-term myeloid lineage skewing [3,19]. As shown in Figure 4B, BM from RTA 408 rescued donors was able to establish robust hematopoietic engraftment in primary hosts. Moreover, RTA 408 treated BM sustained long-term, multilineage hematopoiesis for 6 months post-transplant (Figure 4C), consistent with the presence of functional HSCs lacking lineage bias. Phenotypic HSCs ($CD150^{+}$LSK) derived from RTA 408 donors cells were assessed in primary recipient mice BM >6 months post-transplant. For comparison, non-TBI donor cell contribution to BM HSCs in primary recipients was evaluated. Importantly, the frequency of $CD150^{+}$LSK cells derived from RTA 408-mitigated donor cells was the same as that derived from non-TBI donor cells (Figure 4D-E). In addition, RTA 408-mitigated BM had the same proportion of $CD150^{+}$ cells within the LSK subset as BM from non-TBI donors, providing further evidence of sustained HSC lineage balance in RTA 408-mitigated BM.

To stringently test functional HSC activity, serial transplantation was performed (Figure 4F). RTA 408 treated BM gave rise to multilineage, donor cell engraftment in all secondary recipients providing direct evidence for HSC self-renewal activity (Figure 4F-G). Consistent with our finding that phenotypic HSC in RTA 408-mitigated BM lack a myeloid-bias, we found a similar overall contribution of control donor cells and RTA 408 donor cells to the total number of circulating myeloid cells (Figure 4G). These data confirm that RTA 408 supports the regeneration of bona fide, functionally competent, lineage-balanced, long-term HSC following exposure to bone marrow-lethal doses of radiation.

Discussion

The results of our studies are consistent with a previous report demonstrating the CDDO variant CDDO-Me, beginning 24 hours after exposure to 7.5 Gy TBI, enhances hematologic recovery and results in 20% survival [13]. Here, we show that the triterpenoid RTA 408 can prevent death caused by hematopoietic acute radiation syndrome in 60% of mice that received 7.5 Gy TBI. Moreover, the administration of just three doses of RTA 408 beginning 24 hours post radiation exposure was sufficient to restore hematopoietic stem and progenitor cell frequency and function to levels seen in non-irradiated mice. The combined results from these studies strongly suggest that RTA 408 and other related triterpenoids are promising candidates that should be evaluated further for the pharmacological treatment of hematopoietic acute radiation syndrome in additional pre-clinical studies.

The mechanism(s) underlying the regenerative effect that RTA 408 on radiation-damaged hematopoietic cells are obscured by the multiplicity of molecular targets of thiol modifying compounds. Relevant targets include JAK/STAT3 [23] and canonical NF-kB signaling pathways [11] both of which are reportedly inhibited by triterpenoids. In addition, triterpenoids induce Nrf2-dependent transcription of a plethora of antioxidant enzymes by disrupting the interaction of Nrf2 with its inhibitor Keap1, thereby preventing the proteolytic degradation of Nrf2 and facilitating its nuclear translocation [9,10,24]. Nfr2 has radioprotective activity in the hematopoietic system [13], lending support to the hypothesis that induction of antioxidant enzymes is critical for the bone marrow-protective effects of triterpenoids, including RTA 408. However, it is also likely that triterpenoids are activating additional signaling pathways that also make a significant contribution to the regenerative process. For example, CDDO derivatives have been shown to skew the differentiation of myelomonocytic cells in an Erk1/2 and SMAD-dependent manner [25]. Furthermore, CDDO induces granulocytic differentiation of HL-60 cells presumably through induction of CCAAT enhancer-binding protein alpha (CEBPA), a transcription factor critical for granulocytic differentiation [26,27]. The marked increase in circulating neutrophils in RTA 408-mitigated mice (Fig. 2) is consistent with these previous findings. These results suggest that the complex effects of synthetic triterpenoids on multiple signaling pathways regulate hematopoietic cell survival and differentiation.

Acknowledgements

We are grateful to REATA Pharmaceuticals for providing RTA 408 and thank Carly Hernandez for technical support. This work was supported by the NIH (U19 AI091175; C.G., U.R., W.H.F), REATA Pharmaceuticals (U.R.) and the Department of Defense (W81XWH-12-1-0477; U.R.).

References

1. Chao NJ (2007) Accidental or intentional exposure to ionizing radiation: biodosimetry and treatment options. Exp Hematol 35: 24-27.
2. Mauch P, Constine L, Greenberger J, Knospe W, Sullivan J, et al. (1995) Hematopoietic stem cell compartment: acute and late effects of radiation therapy and chemotherapy. Int J Radiat Oncol Biol Phys 31: 1319-1339.
3. Shao L, Luo Y, Zhou D (2014) Hematopoietic stem cell injury induced by ionizing radiation. Antioxid Redox Signal 20: 1447-1462.
4. Xiao M, Whitnall MH (2009) Pharmacological countermeasures for the acute radiation syndrome. Curr Mol Pharmacol 2: 122-133.
5. Suh N, Wang Y, Honda T, Gribble GW, Dmitrovsky E, et al. (1999) A novel synthetic oleanane triterpenoid, 2-cyano-3,12-dioxoolean-1,9-dien-28-oic acid, with potent differentiating, antiproliferative, and anti-inflammatory activity. Cancer Res 59: 336-341.
6. Yates MS, Tran QT, Dolan PM, Osburn WO, Shin S, et al. (2009) Genetic versus chemoprotective activation of Nrf2 signaling: overlapping yet distinct gene expression profiles between Keap1 knockout and triterpenoid-treated mice. Carcinogenesis 30: 1024-1031.
7. Auletta JJ, Alabran JL, Kim BG, Meyer CJ, Letterio JJ (2010) The synthetic triterpenoid, CDDO-Me, modulates the proinflammatory response to in vivo lipopolysaccharide challenge. J Interferon Cytokine Res 30: 497-508.
8. Place AE, Suh N, Williams CR, Risingsong R, Honda T, et al. (2003) The novel synthetic triterpenoid, CDDO-imidazolide, inhibits inflammatory response and tumor growth in vivo. Clin Cancer Res 9: 2798-2806.

9. Liby K, Hock T, Yore MM, Suh N, Place AE, et al. (2005) The synthetic triterpenoids, CDDO and CDDO-imidazolide, are potent inducers of heme oxygenase-1 and Nrf2/ARE signaling. Cancer Res 65: 4789-4798.

10. Thimmulappa RK, Scollick C, Traore K, Yates M, Trush MA, et al. (2006) Nrf2-dependent protection from LPS induced inflammatory response and mortality by CDDO-Imidazolide. Biochem Biophys Res Commun 351: 883-889.

11. Ahmad R, Raina D, Meyer C, Kharbanda S, Kufe D (2006) Triterpenoid CDDO-Me blocks the NF-kappaB pathway by direct inhibition of IKKbeta on Cys-179. J Biol Chem 281: 35764-35769.

12. Daroczi B, Kari G, Ren Q, Dicker AP, Rodeck U (2009) Nuclear factor kappaB inhibitors alleviate and the proteasome inhibitor PS-341 exacerbates radiation toxicity in zebrafish embryos. Mol Cancer Ther 8: 2625-2634.

13. Kim JH, Thimmulappa RK, Kumar V, Cui W, Kumar S, et al. (2014) NRF2-mediated Notch pathway activation enhances hematopoietic reconstitution following myelosuppressive radiation. J Clin Invest 124: 730-741.

14. Zhang DD (2013) Bardoxolone brings Nrf2-based therapies to light. Antioxid Redox Signal 19: 517-518.

15. Reisman SA, Lee CY, Meyer CJ, Proksch JW, Sonis ST, et al. (2014) Topical application of the synthetic triterpenoid RTA 408 protects mice from radiation-induced dermatitis. Radiat Res 181: 512-520.

16. Li B, Bailey AS, Jiang S, Liu B, Goldman DC, et al. (2010) Endothelial cells mediate the regeneration of hematopoietic stem cells. Stem Cell Res 4: 17-24.

17. Goldman DC, Bailey AS, Pfaffle DL, Al Masri A, Christian JL, et al. (2009) BMP4 regulates the hematopoietic stem cell niche. Blood 114: 4393-4401.

18. Ames E, Harouna S, Meyer C, Welniak LA, Murphy WJ (2012) The triterpenoid CDDO-Me promotes hematopoietic progenitor expansion and myelopoiesis in mice. Biol Blood Marrow Transplant 18: 396-405.

19. Chua HL, Plett PA, Sampson CH, Joshi M, Tabbey R, et al. (2012) Long-term hematopoietic stem cell damage in a murine model of the hematopoietic syndrome of the acute radiation syndrome. Health Phys 103: 356-366.

20. Shao L, Feng W, Li H, Gardner D, Luo Y, et al. (2014) Total body irradiation causes long-term mouse BM injury via induction of HSC premature senescence in an Ink4a- and Arf-independent manner. Blood 123: 3105-3115.

21. Simonnet AJ, Nehme J, Vaigot P, Barroca V, Leboulch P, et al. (2009) Phenotypic and functional changes induced in hematopoietic stem/progenitor cells after gamma-ray radiation exposure. Stem Cells 27: 1400-1409.

22. Kiel MJ, Yilmaz OH, Iwashita T, Yilmaz OH, Terhorst C, et al. (2005) SLAM family receptors distinguish hematopoietic stem and progenitor cells and reveal endothelial niches for stem cells. Cell 121: 1109-1121.

23. Ahmad R, Raina D, Meyer C, Kufe D (2008) Triterpenoid CDDO-methyl ester inhibits the Janus-activated kinase-1 (JAK1)-->signal transducer and activator of transcription-3 (STAT3) pathway by direct inhibition of JAK1 and STAT3. Cancer Res 68: 2920-2926.

24. Thimmulappa RK, Fuchs RJ, Malhotra D, Scollick C, Traore K, et al. (2007) Preclinical evaluation of targeting the Nrf2 pathway by triterpenoids (CDDO-Im and CDDO-Me) for protection from LPS-induced inflammatory response and reactive oxygen species in human peripheral blood mononuclear cells and neutrophils. Antioxid Redox Signal 9: 1963-1970.

25. Ji Y, Lee HJ, Goodman C, Uskokovic M, Liby K, et al. (2006) The synthetic triterpenoid CDDO-imidazolide induces monocytic differentiation by activating the Smad and ERK signaling pathways in HL60 leukemia cells. Mol Cancer Ther 5: 1452-1458.

26. Konopleva M, Tsao T, Ruvolo P, Stiouf I, Estrov Z, et al. (2002) Novel triterpenoid CDDO-Me is a potent inducer of apoptosis and differentiation in acute myelogenous leukemia. Blood 99: 326-335.

27. Koschmieder S, D'Alo F, Radomska H, Schoneich C, Chang JS, et al. (2007) CDDO induces granulocytic differentiation of myeloid leukemic blasts through translational up-regulation of p42 CCAAT enhancer binding protein alpha. Blood 110: 3695-3705.

Figure Legends

Figure 1. Mice treated with RTA 408 24 hours post TBI survive lethal BM-lethal doses of radiation.

(A) Experimental schema. Mice exposed to 7-8 Gy TBI were injected i.p. with 17.5 mg/kg RTA 408 per day beginning 24 hours post TBI. Mice were monitored for survival through day 35. Complete blood counts (CBC) and bone marrow analysis was performed at the indicated time points. (B-D) Survival of TBI mice following RTA 408 or vehicle only treatment. In (B), N=5 mice per treatment group and for (C-D), N=10 mice per treatment group. Statistically significant differences between survival distributions were determined by log-rank test. (*P<0.05; ****P<0.0001; ns: not significant).

Figure 2. Hematological recovery in RTA 408 treated 7.5 Gy TBI mice.

(A) Circulating blood cell (CBC) analysis in RTA 408 treated 7.5 Gy TBI mice 2 weeks and 11 weeks post TBI. Pooled results from n=7-8 mice are shown. CBCs from control, non-TBI mice (n=6) are also shown. WBC: white blood cells; RBC: red blood cells. Although platelets are significantly higher in RTA 408-treated mice, they are still within normal range. (B) Nucleated bone marrow cell counts in 7.5 Gy TBI mice treated with RTA 408 (n=8) 14 weeks post TBI and age matched, non-TBI controls (n=5). A Student's t-test was used for statistical analysis and * indicates P<0.05. For all graphs, error bars indicate S.E.M.

Figure 3. Restoration of hematopoietic stem and progenitor cell frequency in RTA 408-mitigated 7.5 Gy TBI mice to non-TBI levels.

(A) Representative flow cytometry analysis of 7.5Gy TBI + RTA 408 mice and age-matched control BM, 14 weeks post TBI. Parental populations are indicated on the top of each plot and gates used for analysis are shown. (B) Calculated frequency of hematopoietic progenitor populations based on flow cytometry analysis. No significant differences between control non-TBI (n=5) and 7.5 Gy TBI +RTA 408 (n=8) mice were observed. (C) Comparison of in vitro colony forming unit activity in methylcellulose supplemented with IL3, IL6, TPO and SCF. Total colonies per input BM and types of colonies formed were not different between RTA 408-mitigated

BM (n=6) and age-matched non-TBI BM (n=5). BFU-E: burst forming unit erythroid; GEMM: mixed lineage granulocytic, erythroid, macrophage, megakaryocyte; G/M/GM: myeloid colonies containing granulocytes (G), macrophages (M) or both cell types (GM). (D) $CD150^{+}$LSK cell frequency in RTA 408-mitigated TBI mice (n=8) is the same as in non-TBI, age-matched mice (n=5). (E) Similar $CD150^{+}$ cell frequency in the LSK compartments of RTA 408-mitigated BM and non-TBI BM. Unpaired student's t-tests were used for statistical analysis. Error bars indicate SEM.

Figure 4. Treatment with RTA 408 restores functional HSC in 7.5 Gy TBI mice.

(A) Primary transplant schema. Donor cells from 4 individual 7.5 Gy donor TBI + RTA 408 mice were transplanted into 4 cohorts of 2-3 recipient mice. Flow cytometry analysis was used to evaluate blood lineages and distinguish donor, host and competitor cells. B) Contribution of 7.5 Gy TBI + RTA 408 donor BM cells to peripheral blood leukocytes following transplant over time. Pooled results from 10-11 recipient mice are shown. C) Lineage analysis of circulating donor cells derived from TBI + RTA 408 BM 6 months following transplant. Donor cells from TBI + RTA 408 BM contributed to both myeloid ($Mac1^{+}$ and/or $Gr1^{+}$) and lymphoid ($B220^{+}$ B-cells, $CD3^{+}$ T-cells) lineages. Pooled results from 10-11 recipient mice are shown. (D-F) Donor cell analysis in BM >6 months following transplantation. Recipient mice (n=3) transplanted with TBI + RTA 408 BM from 3 different donors were analyzed. A separate cohort of mice (n=3) that received BM from 2 non-TBI donors was used for controls. (D) Similar levels of BM donor cell engraftment by non-TBI donor cells and 7.5 Gy TBI+ RTA 408 donor cells. (E) Similar contribution to CD150+LSK cells by non-TBI donor cells and 7.5 Gy TBI+ RTA 408 donor cells. (F) The same proportion of $CD150^{+}$ cells in the LSK compartment were derived from non-TBI donor cells or TBI+ RTA 408 donor cells. (G) Secondary transplant schema. BM from two primary recipient mice reconstituted with non-TBI or 7.5Gy TBI + RTA 408 donor cells were serially transplanted into cohorts of 4-5 secondary recipients. (H) Peripheral blood analysis of secondary recipient mice 16 weeks post-transplant.

Figure 1
Goldman et al

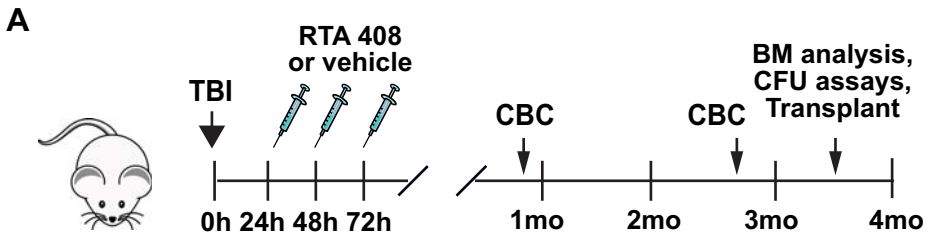

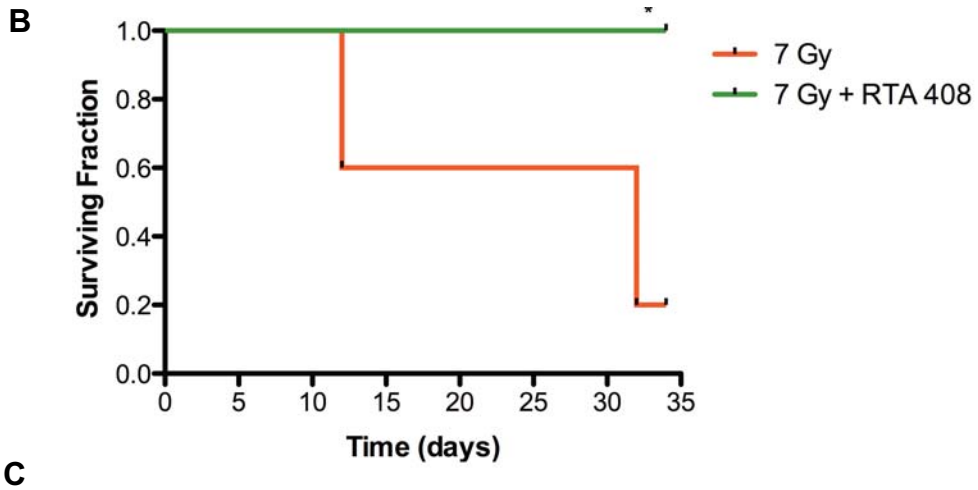

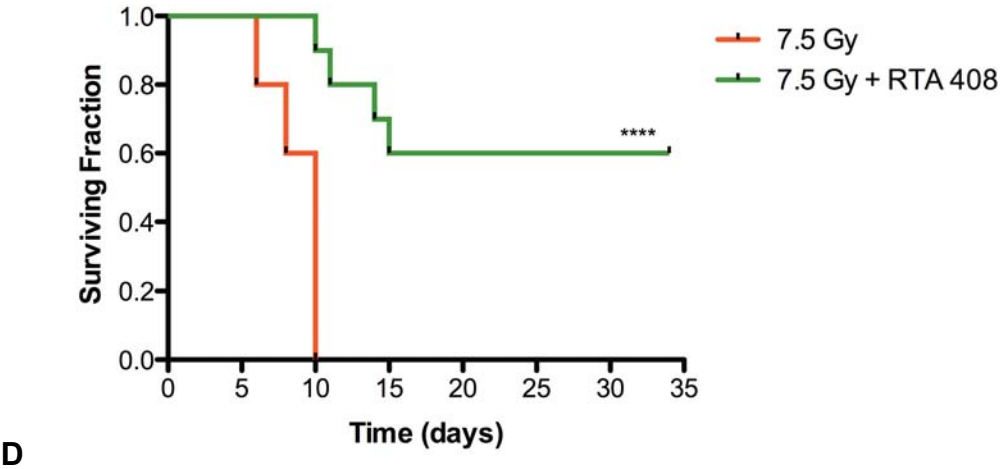

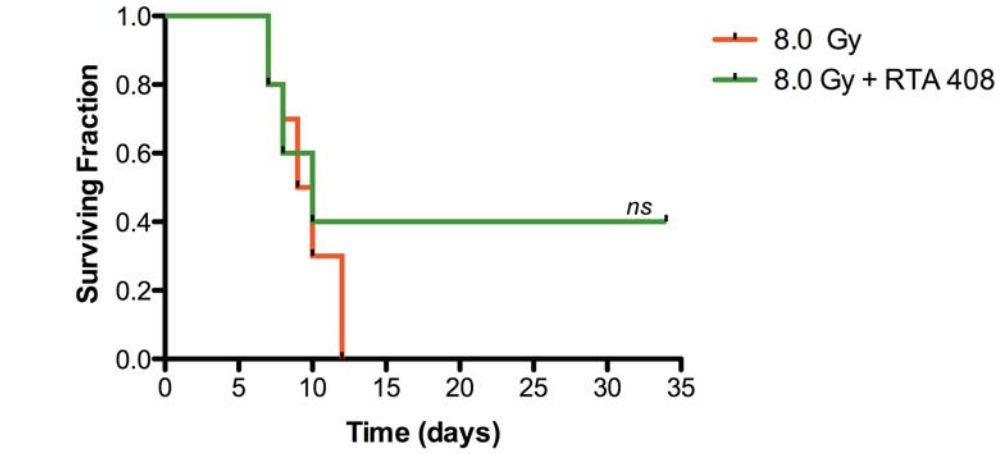

Figure 2
Goldman et al

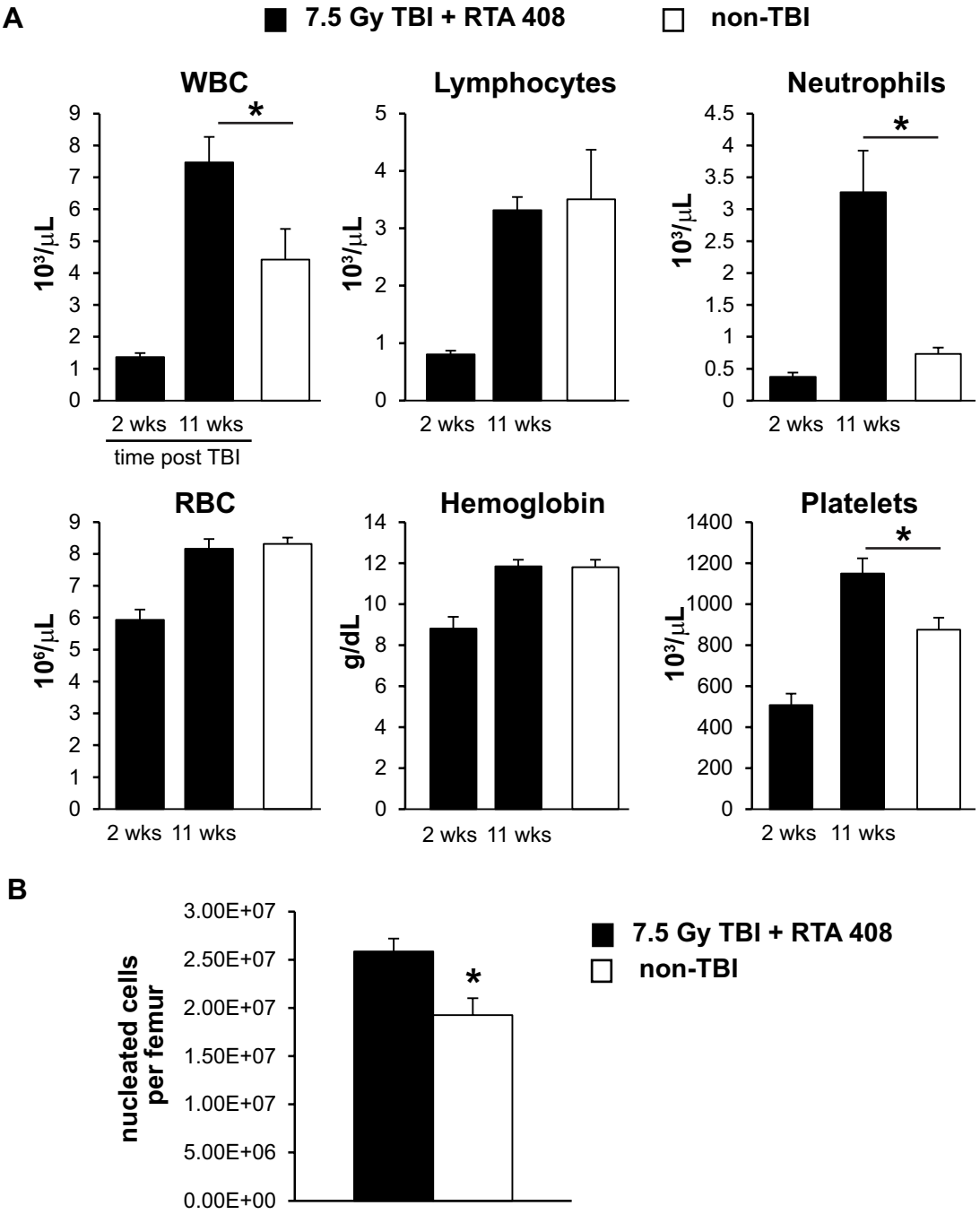

Figure 3
Goldman et al

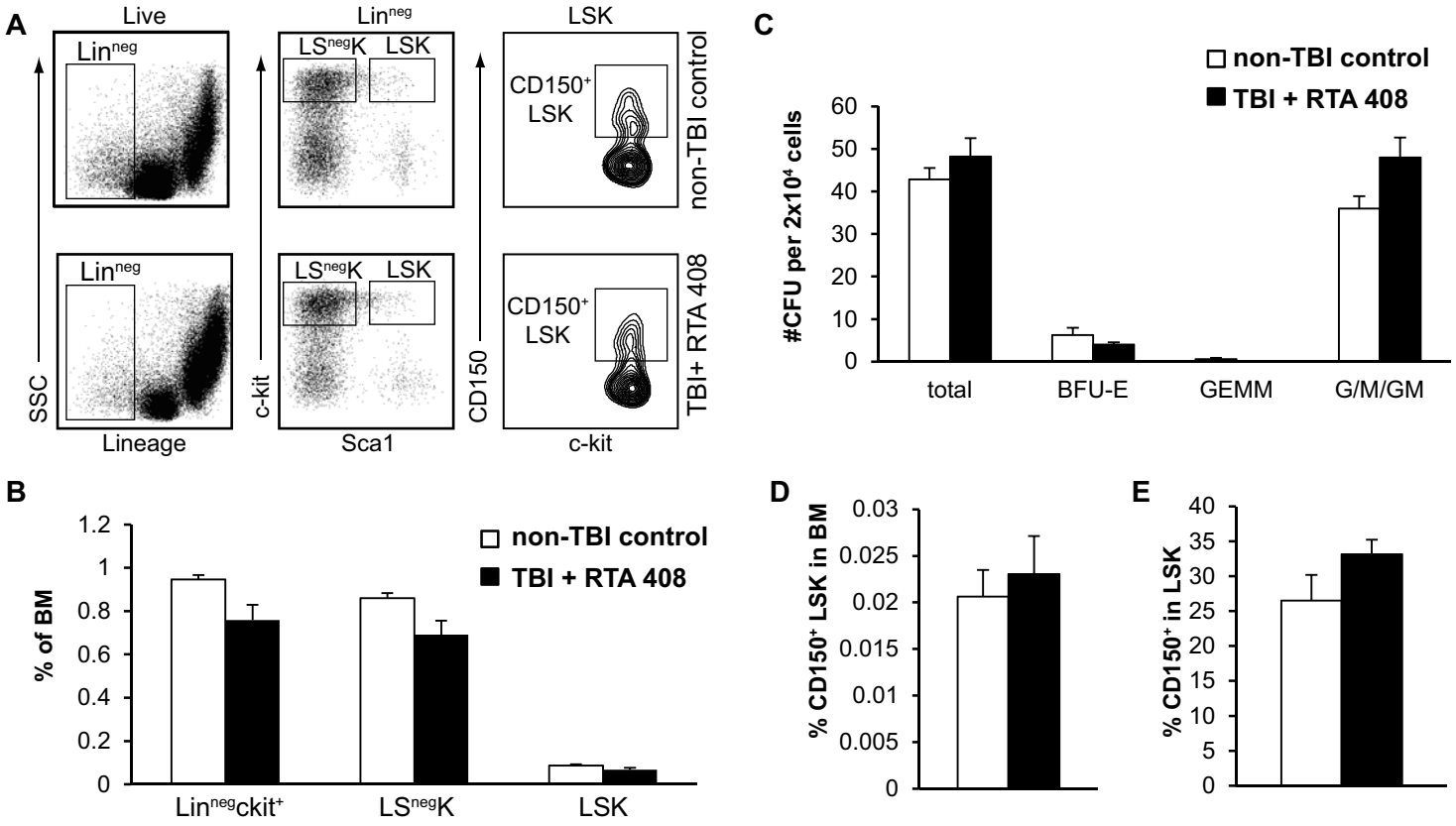

Figure 4
Goldman et al